U.S. Department
of Transportation
Federal Railroad
Administration

Office of Research,
Development and Technology
Washington, DC 20590

Load Environment Characterization of Tank Car Stub Sill During Revenue Operations

DOT/FRA/ORD-23/34

Final Report | September 2023

REPORT DOCUMENTATION PAGE

Form Approved
OMB No. 0704-0188

1. AGENCY USE ONLY (Leave blank)	2. REPORT DATE	3. REPORT TYPE AND DATES COVERED
	April 2023	Technical Report

4. TITLE AND SUBTITLE

Load Environment Characterization of Tank Car Stub Sill During Revenue Operations

5. FUNDING NUMBERS

6. AUTHOR(S)

Timothy Martin ORCID 0000-0002-5280-3142

7. PERFORMING ORGANIZATION NAME(S) AND ADDRESS(ES)

ENSCO, Inc
5400 Port Royal Rd.,
Springfield, VA 22151

8. PERFORMING ORGANIZATION REPORT NUMBER

SERV-REPT-0003074

9. SPONSORING/MONITORING AGENCY NAME(S) AND ADDRESS(ES)

U.S. Department of Transportation
Federal Railroad Administration
Office of Railroad Policy and Development
Office of Research and Development
Washington, DC 20590

10. SPONSORING/MONITORING AGENCY REPORT NUMBER

DOT/FRA/ORD-23/34

11. SUPPLEMENTARY NOTES

COR: Francisco González, III

12a. DISTRIBUTION/AVAILABILITY STATEMENT

This document is available to the public through the FRA Web site at http://www.fra.dot.gov.

12b. DISTRIBUTION CODE

13. ABSTRACT (Maximum 200 words)

Fractures in the stub sills of tank cars pose a significant problem for the rail industry due to the potential for damage to the tank structure and possible release of the contents. Previous FRA research revealed that high magnitude coupling forces that occur in yard operations have the potential to exceed yield limits of mild steel. A research team conducted a cooperative test program to characterize coupling loads for tank cars in yard operations. In a continuation of this research, the team evaluated revenue service for both main and yard operations for 10 months and 14,000 miles. The testing showed that the train dynamics from mainline and yard operations are nearly equally important for longitudinal coupler forces and the resulting stub sill strains.

14. SUBJECT TERMS

Tank Cars, Rail, Stub Sill Failures, Impact Test, Yard Operation, Mainline Operation, Main Operation, Car Coupling, Draft Gear, Instrumented Couplers

15. NUMBER OF PAGES

50

16. PRICE CODE

17. SECURITY CLASSIFICATION OF REPORT	18. SECURITY CLASSIFICATION OF THIS PAGE	19. SECURITY CLASSIFICATION OF ABSTRACT	20. LIMITATION OF ABSTRACT
Unclassified	Unclassified	Unclassified	

NSN 7540-01-280-5500

Standard Form 298 (Rev. 2-89)
Prescribed by ANSI Std. 239-18
298-102

METRIC/ENGLISH CONVERSION FACTORS

ENGLISH TO METRIC	METRIC TO ENGLISH
LENGTH (APPROXIMATE)	**LENGTH (APPROXIMATE)**
1 inch (in) = 2.5 centimeters (cm)	1 millimeter (mm) = 0.04 inch (in)
1 foot (ft) = 30 centimeters (cm)	1 centimeter (cm) = 0.4 inch (in)
1 yard (yd) = 0.9 meter (m)	1 meter (m) = 3.3 feet (ft)
1 mile (mi) = 1.6 kilometers (km)	1 meter (m) = 1.1 yards (yd)
	1 kilometer (km) = 0.6 mile (mi)
AREA (APPROXIMATE)	**AREA (APPROXIMATE)**
1 square inch (sq in, in^2) = 6.5 square centimeters (cm^2)	1 square centimeter (cm^2) = 0.16 square inch (sq in, in^2)
1 square foot (sq ft, ft^2) = 0.09 square meter (m^2)	1 square meter (m^2) = 1.2 square yards (sq yd, yd^2)
1 square yard (sq yd, yd^2) = 0.8 square meter (m^2)	1 square kilometer (km^2) = 0.4 square mile (sq mi, mi^2)
1 square mile (sq mi, mi^2) = 2.6 square kilometers (km^2)	10,000 square meters (m^2) = 1 hectare (ha) = 2.5 acres
1 acre = 0.4 hectare (he) = 4,000 square meters (m^2)	
MASS - WEIGHT (APPROXIMATE)	**MASS - WEIGHT (APPROXIMATE)**
1 ounce (oz) = 28 grams (gm)	1 gram (gm) = 0.036 ounce (oz)
1 pound (lb) = 0.45 kilogram (kg)	1 kilogram (kg) = 2.2 pounds (lb)
1 short ton = 2,000 pounds (lb) = 0.9 tonne (t)	1 tonne (t) = 1,000 kilograms (kg)
	= 1.1 short tons
VOLUME (APPROXIMATE)	**VOLUME (APPROXIMATE)**
1 teaspoon (tsp) = 5 milliliters (ml)	1 milliliter (ml) = 0.03 fluid ounce (fl oz)
1 tablespoon (tbsp) = 15 milliliters (ml)	1 liter (l) = 2.1 pints (pt)
1 fluid ounce (fl oz) = 30 milliliters (ml)	1 liter (l) = 1.06 quarts (qt)
1 cup (c) = 0.24 liter (l)	1 liter (l) = 0.26 gallon (gal)
1 pint (pt) = 0.47 liter (l)	
1 quart (qt) = 0.96 liter (l)	
1 gallon (gal) = 3.8 liters (l)	
1 cubic foot (cu ft, ft^3) = 0.03 cubic meter (m^3)	1 cubic meter (m^3) = 36 cubic feet (cu ft, ft^3)
1 cubic yard (cu yd, yd^3) = 0.76 cubic meter (m^3)	1 cubic meter (m^3) = 1.3 cubic yards (cu yd, yd^3)
TEMPERATURE (EXACT)	**TEMPERATURE (EXACT)**
[(x-32)(5/9)] °F = y °C	[(9/5) y + 32] °C = x °F

QUICK INCH - CENTIMETER LENGTH CONVERSION

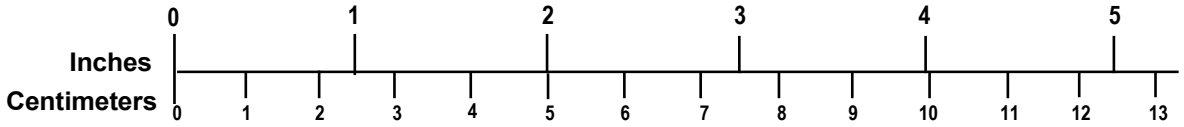

QUICK FAHRENHEIT - CELSIUS TEMPERATURE CONVERSIO

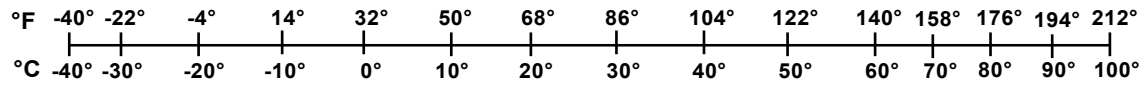

For more exact and or other conversion factors, see NIST Miscellaneous Publication 286, Units of Weights and Measures. Price $2.50 SD Catalog No. C13 10286

Updated 6/17/98

Acknowledgements

This research team was brought together under the leadership of Mr. Francisco González, III of the Federal Railroad Administration. This study would not have been possible without the generosity of Union Tank for loaning and maintaining the tank car. This study was also made possible by a partner Class I railroad providing most of the movement cost and arrangements.

Contents

Illustrations

Tables

Executive Summary

Fractures in the stub sills of tank cars pose a significant problem for the rail industry due to the potential for damage to the tank structure and possible release of the contents. Previous research revealed that high magnitude coupling forces that occur in yard operations have the potential to exceed yield limits of mild steel and initiate stub sill damage. These high force events in yards could be mitigated if railroads were aware of the limiting combination of coupling speed and impacting mass limits.

In 2018, the Federal Railroad Administration (FRA) sponsored a research team from ENSCO, Inc. (ENSCO) to conduct a series of impact tests for several tank car configurations at various coupling speeds. The objective of this research study was to characterize the load environment on tank cars during yard operations. Researchers instrumented a tank car loaned to FRA by Union Tank with multiple transducers and a data collection system that supported the high sampling rates required for impact testing. The team conducted a series of impact tests simulating various coupling conditions at Amsted Rail's test facility in Camp Hill, PA. Researchers collected over 700 impact tests for various car configurations, end-of-car units, and coupling speeds. The results showed that the coupling speed and the type of end-of-car units employed on the cars have the most influence on the peak longitudinal impact force, whereas anvil and hammer configurations have limited effect on the peak impact force. Results also showed that different end-of-car units exhibited different impact forces within various speed ranges.

In 2022, FRA again sponsored an ENSCO team to conduct a cooperative test program to better characterize the load environment of tank car operations in both mainline and yard operations. Main operations include all train movements as a single consist on mainline, sidings, and yards, and yard operations include all train movements (or impacts) while assembling train consists. Researchers also evaluated how the results from the previous impact test program apply to real revenue service yard operations. Under this effort, the team instrumented the tank car loaned to FRA by Union Tank Car with the same multiple transducers and data collection system used in previous impact testing. The team collected acceleration, force, speed, and strain data continuously over 10 months and 14,000 miles. Researchers conducted a comprehensive statistical data analysis to investigate the effect of different parameters, particularly the effect of mainline versus yard operations. The team drew the following major conclusions from the data analysis:

- Yard operations (1830 kip maximum) had slightly larger longitudinal coupler forces than mainline operations (1000 kip maximum) but similar magnitudes. Longitudinal coupler forces had similar magnitudes for both the autonomous testing and the previous impact testing (1540 kip maximum).
- Vertical coupler forces had similar magnitudes for both main operations (51 kip maximum) and yard operations (58 kip maximum) but about half that of the previous impact testing (117 kip maximum).
- The rosette strains had similar magnitudes overall between main operations (670 με to 1110 με maximums) and yard operations (650 με to 1720 με maximums) with some locations higher and some lower. The rosette strains had similar magnitudes between

autonomous testing and the previous impact testing (570 με to 2440 με maximums) but showed some variation, with some locations higher and some lower.

- The in-board strain location had the highest values for both autonomous testing (1720 με maximum) and the previous impact testing (2440 με maximum).

This testing showed that the train dynamics from mainline and yard operations are nearly equally important for longitudinal coupler forces and the resulting stub sill strains. This finding will help determine important areas of future research and identify recommendations for railroads to improve safety, particularly in improvements to both mainline and yard operation scenarios.

1. Introduction

The Federal Railroad Administration (FRA) sponsored a research team from ENSCO, Inc. (ENSCO) to conduct a cooperative test program on Class I railroads across the United States and gather continuous measurement data on an instrumented tank car during autonomous revenue service in 2022. The data was collected for all train movements including mainline movements and yard operations for train make-up. The team analyzed the test data to better understand the load environment of tank car stub sills during all aspects of operations and to determine where the highest forces and strains occur.

1.1 Background

The industry has observed fractures on stub sill tank cars for many years. Undetected, these fractures can develop into a variety of tank car failures. While tank car ruptures are relatively rare, the potential for a catastrophic HAZMAT release has made these fractures a critical issue within the industry. To address this issue, the industry has implemented special requirements for the construction, inspection, and repair of tank cars.

Research into the underlying cause of tank car stub sill crack initiation and propagation continues. It is believed that the fractures are initiated by discrete events resulting in high stresses. Previous research studies conducted by FRA (Sundaram, 2014) revealed that high magnitude coupling forces that occur in yard operations have the potential to exceed yield limits of mild steel. Stub sill failures were primarily attributed to initial damage from high forces generated in yards, followed by crack propagation resulting from high vertical coupler force events during mainline operations. High-force events in yards could be mitigated with a better understanding of the contributing factors to these high impact loadings during yard operations.

Examples of stub sill fractures observed by CSX Transportation are shown in Figure 1 and Figure 2. These fractures are catastrophic in nature. However, the industry has improved weld design so that the weld between the head brace and stub sill should fail before the weld between the pad and tank.

Figure 1. Stub Sill Fracture Observed in Callahan, FL, from December 2009 (Sundaram, 2014)

Figure 2. Stub Sill Fracture Observed in Charleston, WV, from January 2010 (Sundaram, 2014)

To better characterize the load environment of tank car operations in yards, a research team conducted a cooperative test program at Amsted Rail's test facility in Camp Hill, PA, in 2018. Under that effort, the team instrumented a tank car loaned to FRA by Union Tank Car with multiple transducers including accelerometers, instrumented couplers, and strain gauges. Researchers employed a data collection system that supported the high sampling rates required for conducting impact testing and collected impact data for various car configurations, end-of-car units, and coupling speeds. Figure 3 shows the study tank car provided by Union Tank Car. Figure 4 shows a detailed view of the end of the tank car with the stub sill attachment. A previous report by FRA (Meymand, 2019) documented the results of this impact testing.

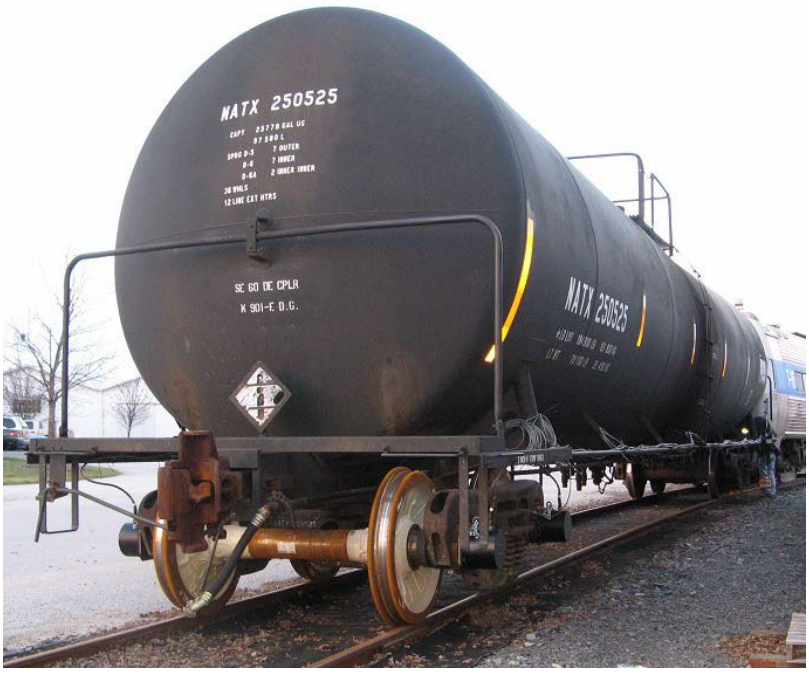

Figure 3. Instrumented Tank Car

Figure 4. Detail View of the Stub Sill and Head Brace Attached to the Tank of the Instrumented Tank Car

The research team determined that the coupling speed and the type of end-of-car units employed on the cars have the most influence on the peak longitudinal impact force, whereas anvil and hammer configurations have limited effect on the peak impact force. The results also showed that the end-of-car unit type has limited effect on the transferred energy between impacting cars, whereas hammer and anvil configurations have considerable effect on the transferred energy. Researchers found that different end-of-car units yielded different impact forces for various speed ranges. Hydraulic cushioning units yielded lower impact forces than both steel friction and elastomer draft gears for all speed ranges, while elastomer draft gears yielded lower impact forces than steel friction draft gears for lower coupling speed ranges.

In 2022, the team conducted a cooperative test program to better characterize the load environment of the tank car operations in both mainline and yards. Researchers also evaluated how the results from the previous impact test program apply to real revenue service yard operations. Under this effort, the team instrumented the tank car with the same multiple transducers and data collection system used in the previous impact testing. Researchers collected continuous data over 10 months and 14,000 miles to ensure that all impacts were recorded.

This report describes the instrumentation, calibration, and testing efforts used in this study and provides analysis of the results and findings.

1.2 Objectives

The objective of this research study was to characterize the load environment on tank cars during mainline and yard revenue operations. The main focus of the study was to identify whether mainline or yard operations had higher impact forces and caused more damage to tank car stub sills.

1.3 Overall Approach

The team conducted a cooperative test program on Class I railroads across the United States in 2022. A tank car loaned to FRA by Union Tank Car was instrumented with multiple transducers and a data collection system that supported the high sampling rates required for conducting revenue testing. The tank car ran in normal revenue service for ten months and covered 14,000 miles of track. Thirty data channels were recorded, including acceleration, force, speed, and strain data. A comprehensive statistical data analysis was conducted to investigate the effect of different parameters in mainline versus yard operations.

1.4 Scope

This study included autonomous revenue service tank car testing with different train handling conditions during mainline and yard operations and the analysis of the collected data.

1.5 Organization of the Report

The test methodology is discussed in Section 2 and includes a review of the instrumented tank car, different sensors used during the test program, and the revenue testing that was conducted. Section 3 presents analysis of the test data, and conclusions are discussed in Section 4.

2. Test Methodology

This section describes the instrumented tank car, the different sensors used during the test program, and the test scenarios used in the revenue testing.

2.1 Instrumented Tank Car

The team instrumented a tank car with multiple transducers and a data collection system that supported the high sampling rates required for autonomous testing. Researchers equipped the instrumented tank car with instrumented couplers on both ends of the car, a vertical coupler force measurement system, multiple accelerometers, and multiple rosette strain gages at various locations around stub sills that were identified as high stress locations by FRA and Union Tank Car subject matter experts. Figure 5 shows a schematic of the test tank car's instrumentation. This is the same instrumentation used in the previous impact test program. During an inspection of the tank car components before the autonomous testing, all of the strain gages originally installed for the impact testing were removed and then re-installed. This strain gage removal was required because it interfered with equipment scanning for fractures in the tank car structure.

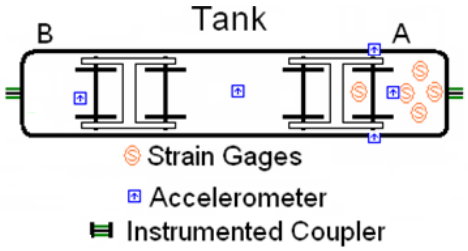

Figure 5. Schematic Diagram of Tank Car's Instrumentation

2.1.1 Coupler Forces

Researchers measured the longitudinal coupler forces on both the A-end and B-end of the tank car. Two instrumented couplers outfitted with strain gauge bridges measured the longitudinal forces. Figure 6 shows an image of instrumented couplers installed on both ends of the car.

Figure 6. Instrumented Couplers for Measuring Longitudinal Coupler Forces (A-End on Left, B-End on Right)

To measure vertical forces, the team mounted a pair of shear strain gauges on each side of the stub sill (Figure 7). The left picture shows the old gauges in black, while the right picture shows the new gauges covered with tape. Researchers wired the shear strain gauges to form a full bridge. The mounting process included grinding and polishing the coupler surface to provide a smooth area to which the strain gages were welded. The team used RTV silicone rubber coatings as protective and waterproofing coatings. Team members applied these shear strain gauges only on the A-end of the instrumented tank car.

Figure 7. Strain Gages Installed on the Stub Sill for Measuring Vertical Coupler Force (Old on Left, New on Right)

2.1.2 Strain Gages

The team installed five sets of rosette strain gauges on various locations around the stub sill on the A-end of the tank car; these locations were identified as high stress areas in consultation with FRA and Union Tank Car's subject matter experts. To determine principal stresses, researchers installed three individual strain gauges 45 degrees apart to form a rosette. Figure 8 shows the rosette strain gauge installed on the shoulder pad centered above the head shoe. The left picture shows the old installation, while the center picture shows the new installation after it has been covered with tape.

Figure 8. Shoulder Pad Strain Gage Installed Above the Head Shoe at the A-End of the Instrumented Tank Car (Old on Left, New in Center)

Figure 9 shows the rosette strain gage installed under the car at the end of the stub sill. This gage is referred to as the in-board strain gage. The left picture shows the old installation, while the center picture shows the new installation after it has been covered with transparent tape.

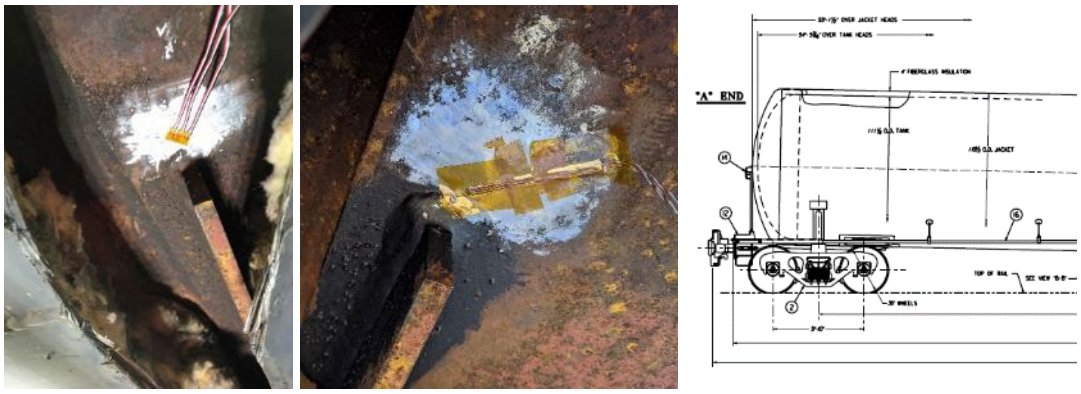

Figure 9. In-Board Strain Gage Installed Under the Car at the End of the Stub Sill Beam (Old on Left, New in Center)

Figure 10 shows the rosette strain gage installed on the head shoe close to a corner weld. This gage is referred to as the head shoe strain gage. The left picture shows the old installation, while the center picture shows the new installation.

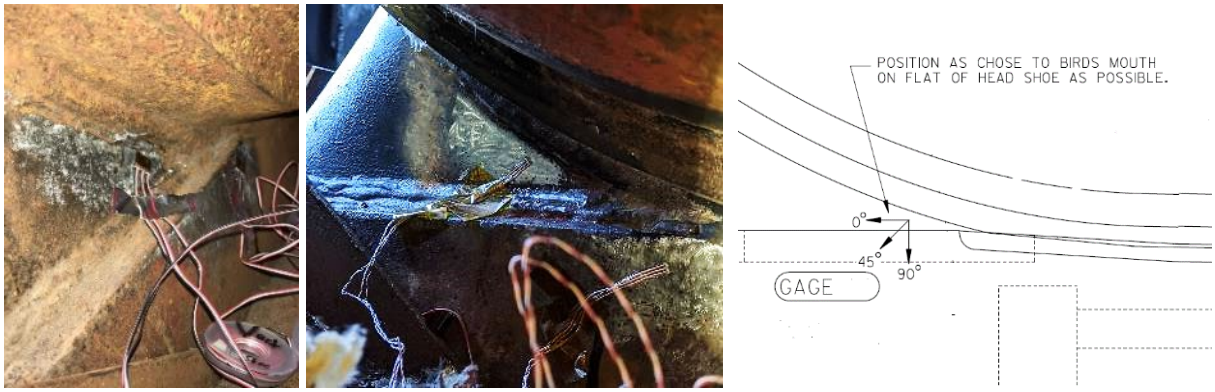

Figure 10. Strain Gage Installed on the Head Shoe Close to the Corner (Old on Left, New in Center)

Figure 11 shows the rosette strain gage installed on the sub sill below the head shoe strain gage close to the draft gear's rear stop. This gage is referred to as the stub sill stop strain gage. The left picture shows the old installation, while the center picture shows the new installation.

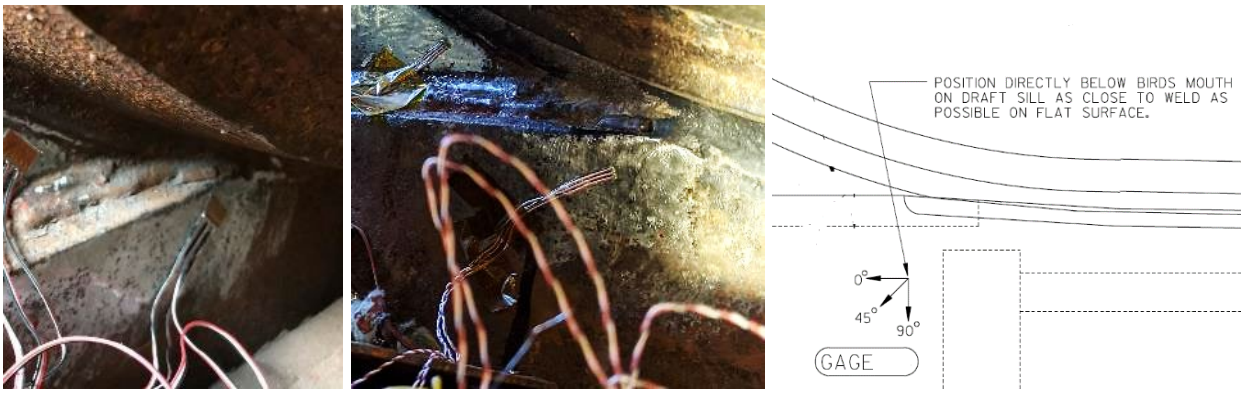

Figure 11. Strain Gage Installed on the Stub Sill Close to the Rear Stop (Old on Left, New in Center)

Figure 12 shows the rosette strain gage installed on top of the sub sill close to the head shoe. This gage is referred to as the head brace strain gage. The left picture shows the old installation, while the center picture shows the new installation after it had been covered with tape.

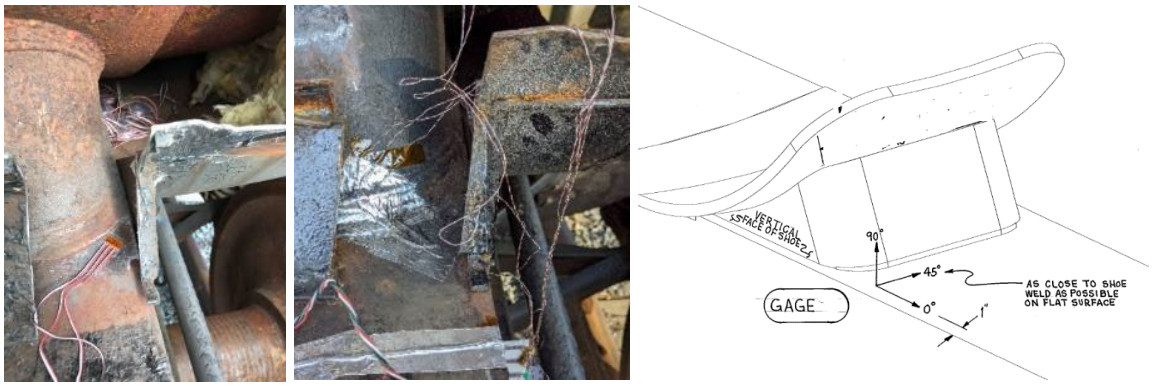

Figure 12. Strain Gage Installed on Top of the Stub Sill Close to the Head Shoe (Old on Left, New in Center)

2.1.3 Accelerometers

The team installed five accelerometers at multiple locations on the tank car. Figure 13 shows a tri-axial accelerometer mounted on top of the carbody to measure accelerations in longitudinal, lateral, and vertical directions. Figure 14 shows two tri-axial accelerometers mounted on the stub sill at each end of the car and one accelerometer mounted to the axle.

Figure 13. Tri-Axial Accelerometer Mounted on Top of the Carbody

Figure 14. Accelerometers Mounted on the Stub Sills and Axle (Stub Sill A-End on Left, Stub Sill B-End in Center, Axle on Right)

2.1.4 Other Transducers

Researchers also mounted a GPS antennae and receiver to collect speed and location information.

2.1.5 Data Acquisition and Hardware Settings

The team collected data using National Instrument's PCIe6353 Data Acquisition Card. The card supported 32 input analog channels with 16-bit resolution, and the collection system recorded 30 channels of data at a rate of 2 kHz. The system used a low-pass, anti-aliasing, fourth order Butterworth filter with a Sallen-Key Topology filter board to filter the input data with a cut-off frequency of 1,000 Hz. A Nuvo-5095GC ruggedized computer collected and stored data through LabView software. The system used +/- 5 V and +/- 12 V power supply to provide clean power to the transducers. Figure 15 shows the junction box that was installed to the side of the tank car. The box contained the computer, acquisition hardware, power supply, analog filter board, and terminal blocks for signal routing and distribution.

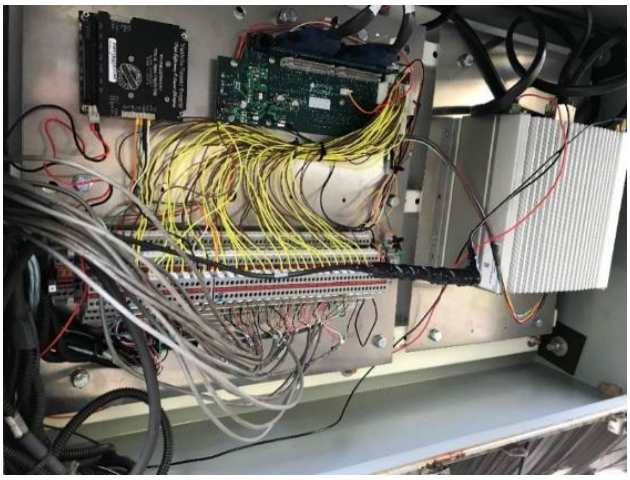

Figure 15. Junction Box with Data Collection System Hardware

Four 115 W, 12 V solar modules, solar panels, and a set of 110 Ah, 12 V AGM batteries powered the system. Figure 16 shows the solar panels and the battery box. The battery box also contained the electronics that controlled battery charging.

Figure 16. Solar Panel and Battery Box on Top of Instrumented Tank Car

2.1.6 Channel Assignments

Table 1 shows assignments and descriptions of each channel. In addition to the channels listed in the table, researchers also collected GPS location and speed.

Table 1. Data Collection System Input Channel List

Channel Number	Description	Units
1	Carbody Longitudinal Acceleration	[g]
2	Carbody Lateral Acceleration	[g]
3	Carbody Vertical Acceleration	[g]
4	Stub Sill B-End Vertical Acceleration	[g]
5	Stub Sill B-End Longitudinal Acceleration	[g]
6	Stub Sill A-End Longitudinal Acceleration	[g]
7	Stub Sill A-End Lateral Acceleration	[g]
8	Axle A-End Right Vertical Acceleration	[g]
9	Stub Sill A-End Vertical Acceleration	[g]
10	Longitudinal Coupler Force A-End	[με]
11	Longitudinal Coupler Force B-End	[με]
12-14	Rosette Strain Gage at Shoulder Pad Location - 45/Vertical/+45	[με]
15	Vertical Coupler Force A-End	[με]
16-18	Rosette Strain Gage at Stub Sill Stop Location – Horizontal/45/Vertical	[με]
19-21	Rosette Strain Gage at Head Shoe Location – Horizontal/45/Vertical	[με]
22-24	Rosette Strain Gage at Head Brace Location – Longitudinal/45/Lateral	[με]
25-27	Rosette Strain Gage at In-Board Location – Longitudinal/45/Lateral	[με]
28-29	Spare Channel	N/A
30	Battery Voltage Monitor	V
31-32	+/- 5 Volt Power Monitor	V

2.1.7 Sensor Calibration

The team calibrated all instrumentation prior to testing and calibrated all portable sensors in a laboratory prior to installation on the vehicle, including accelerometers and longitudinal force bridges on the instrumented couplers. The vertical force bridges on the coupler that converted strains to forces required field calibration.

Researchers calibrated the vertical coupler force in the field using a custom load fixture consisting of a metal frame, a calibrated load cell, and a hydraulic ram to apply vertical loads. Figure 17 shows the calibration fixture when downward (left) and upward (right) vertical forces were applied.

Figure 17. Vertical Coupler Force Calibration Setup (Downward Force on Left, Upward Force on Right)

The team measured the applied force and the strain gauges' full bridge output at several points for both upward and downward loadings. The procedure was conducted three times in each direction. Figure 18 shows a graph of the calibration results for the vertical coupler force.

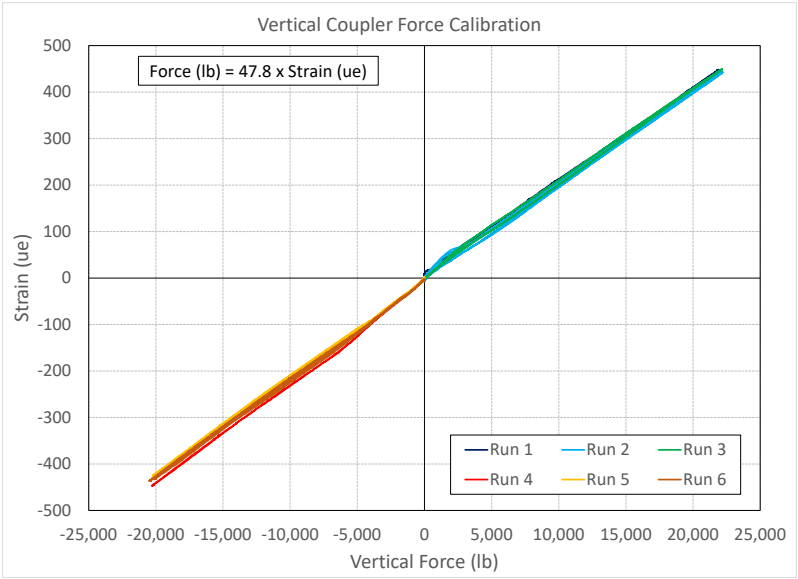

Figure 18. Vertical Coupler Force Calibration Results

2.1.8 Tank Car Weights

Team members filled the tank car with water to the fully loaded condition by weight throughout the program to collect information for the heaviest condition. The fully loaded weight of the car was 263.2 kips, while the empty weight was 78.1 kip.

2.2 Autonomous Test Program

The research team conducted the autonomous test program on two Class I railroads across the United States between March 2022 and December 2022. The test program included a series of railroad moves across portions of the country. Figure 19 shows the instrumented tank car in a yard during the autonomous testing.

Figure 19. Instrumented Tank Car in a Yard During Autonomous Test

At the research team's direction, the railroad put in a request to move the tank car to the next location partway across the country, moving the tank car just like any other car in revenue service. This would typically include shoving the tank car and all the other cars to create the entire train consist, moving the train to the next location, and then breaking down the train at the destination yard. This included multiple starts and stops on the mainline and likely several sidings and yards. Sometimes, this also included stops at yards where the train consist was broken down and a new consist created. Once at the destination, the railroad would put in the next request to move the tank car. This process continued to ensure that data collected covered an adequate cross section of the country.

The team analyzed all data collected including the originally planned route and the additional testing added later. The entire test program collected 14,000 miles of data over 10 months. Each data file collected 30 minutes of continuous data regardless of train movement or forces to ensure that all events were recorded.

Throughout the testing, team members remotely monitored the data to ensure that the data collection system was working correctly. Researchers traveled to the tank car three times to

download the collected data, inspect the instrumentation, and make any needed repairs at two intermediate waypoint locations and the final destination.

2.3 Issues Encountered During Testing

The team encountered several minor issues during the testing:

- The system froze twice. The railroad was able to restart the system at the next destination and testing was able to proceed following the restart.
- The carbody triaxial accelerometer did not produce reliable measurements throughout the testing. This sensor was not used in the analysis.
- Several strain gauges had some intermittent issues that were traced back to corrosion on the bridge completion cards. The team replaced these bridge completion cards during the testing. The worst sensors lost about 1.4 percent of their data.
- The shoulder pad strain gauge (in vertical direction) stopped working toward the end of the testing. Approximately 36 percent of the data for this sensor was lost.
- One of the instrumented couplers had water in the connecter, losing about 0.9 percent of its data.

These issues did not affect the overall test results.

3. Autonomous Test Data Analysis and Results

This section provides an overview of the collected data analysis results. The team first filtered the data to remove invalid data and noise, then conducted a statistical analysis to study the effect of different parameters on the stub sill and coupling behavior. Researchers assessed the peak longitudinal impact force measured by the instrumented coupler as well as the strains and other sensors. These are discussed in detail in the following sections.

3.1 Filtering Data

The research team processed the collected data to filter out invalid data and noise. First, researchers manually and visually checked all the recorded data to remove any invalid data associated with failures of the power system, data collection system, or individual sensors. After manual review of the data, team members filtered the data to remove noise. The data collection sampling rate during testing was 2 kHz. The system was equipped with an analog anti-aliasing fourth order Butterworth low pass filter with a cut-off frequency of 1 kHz. Then the recorded data was further filtered with a digital second order Butterworth low pass filter at 60 Hz. This filter setting was based on results from the previous impact testing where various cut-off frequencies for the digital low pass filter were investigated.

3.2 Initial Analysis

The purpose of the initial analysis was to review all data files for quality, applicability, and value. The initial analysis focused on three areas:

- Determining the operation type for each file
- Finding the maximum values for all channels in each file
- Plotting all channels for every file

The first step was to evaluate the type of operation for each file (i.e., the type of movement, either mainline movement or yard coupling movement). For this report, mainline movement consists of all train movements as a single consist including on mainline, sidings, and yards. Yard movement consists of all train movements (i.e., impacts) in switching yards while assembling or disassembling train consists. These two types of movements are referred to as main and yard operations in this report.

To determine if the movement was main or yard operation, the team mapped the GPS coordinates to see if the location was in a yard. If the tank car experienced many short movements in a yard location, this was considered yard operation for this analysis. On the other hand, if the tank car merely stopped at a single location in a yard, this was considered main operation for this analysis since no coupling action occurred. Figure 20 shows a plot of the type of operation by date for the entire testing period. Note that much of the time was spent in yards waiting to be put in a different consist.

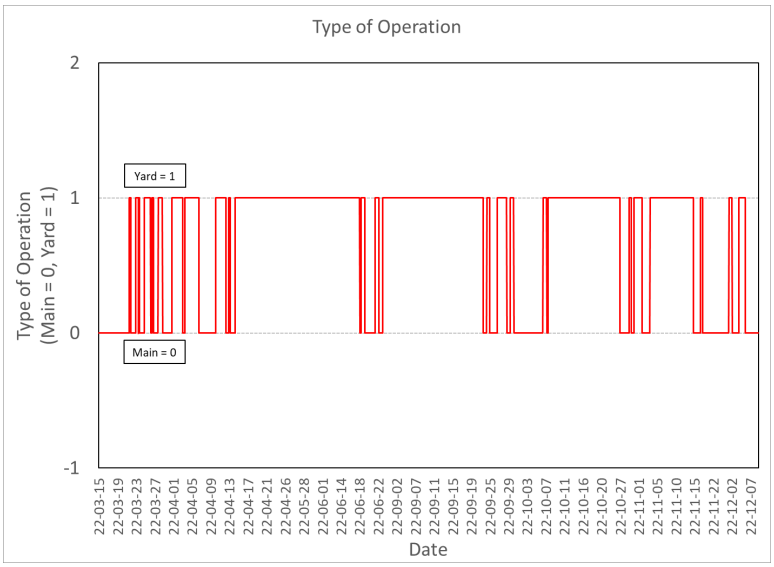

Figure 20. Type of Operation (or Movement) for the Entire Test

Researchers saved the maximum and minimum values for all channels for each data file to a summary file. This summary was used to determine which individual data files were of most interest for further evaluation. Large forces, strains, and accelerations were of particular interest. The operation type from the previous step was also incorporated into this summary file.

The team plotted all channels from each data file. Figure 21 shows an example of these plots from the data file with the largest longitudinal coupler force. By using the summary file and the individual file plots, each file was evaluated to determine whether the data it contained was good or bad. If there was a bad channel in a particular file, only that channel was excluded for that file. After reviewing all data files, it was determined that most of the data was good with a few exceptions (as noted in Section 2.3).

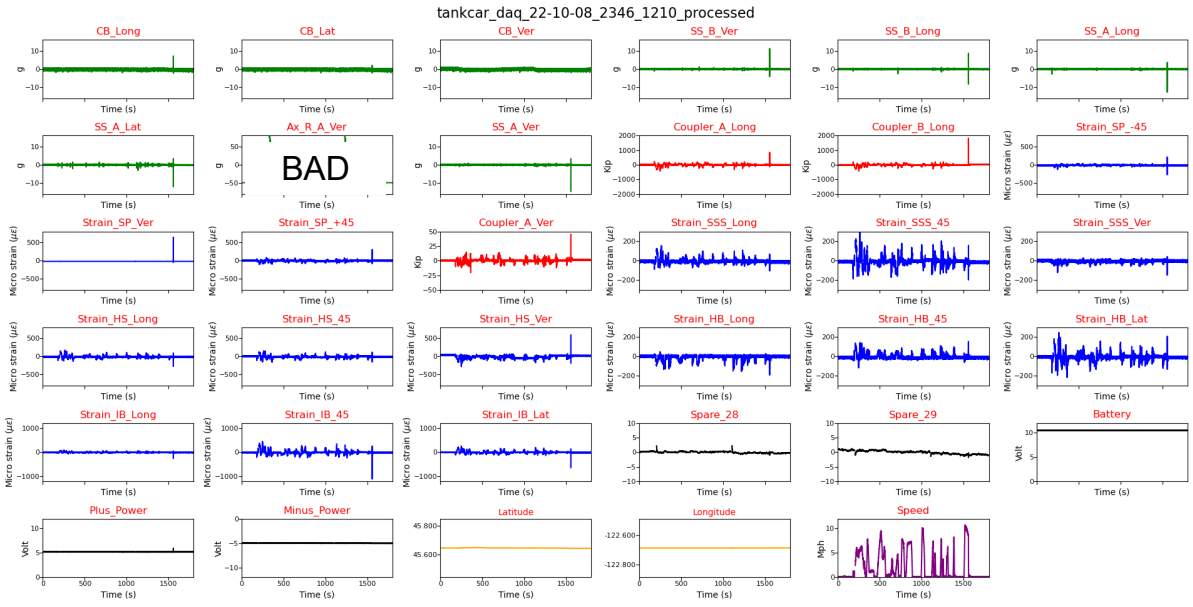

Figure 21. Plot with Highest Yard Longitudinal Coupler Forces (Yard 1, Full File)

3.3 Analysis of Worst Locations

Once all bad or questionable data were eliminated, the analysis focused on investigating locations with the highest values. Data from main and yard operations were analyzed separately. The peak longitudinal coupler forces were approximately the same magnitudes for main and yard operations. The yard operations had the highest overall forces and the highest compression (i.e., positive) forces, which appear to be caused by coupling actions. The main operations had the highest tension (i.e., negative) forces with similar magnitude compression forces, which appear to be caused by train acceleration and breaking actions.

Figure 21 plots 30 minutes for all channels from a sample file with the highest longitudinal coupler forces. Figure 22 shows a highly magnified view of the peak signals from the same file. These plots show the accelerations in green, forces in red, strains in blue, and speed in purple. The speed signal shows many short movements from 0 to 10 mph. This is indicative of yard movements while the railroad assembles the train consist. These plots show many peaks in the forces, acceleration, and strains corresponding to these movements. The magnified view shows the biggest peak in the longitudinal coupler force at approximately 1556 seconds. This corresponds to a sudden drop in speed which was probably caused by the yard impact during the assembly of the train consist. Most of the other channels also show significant peaks at this point.

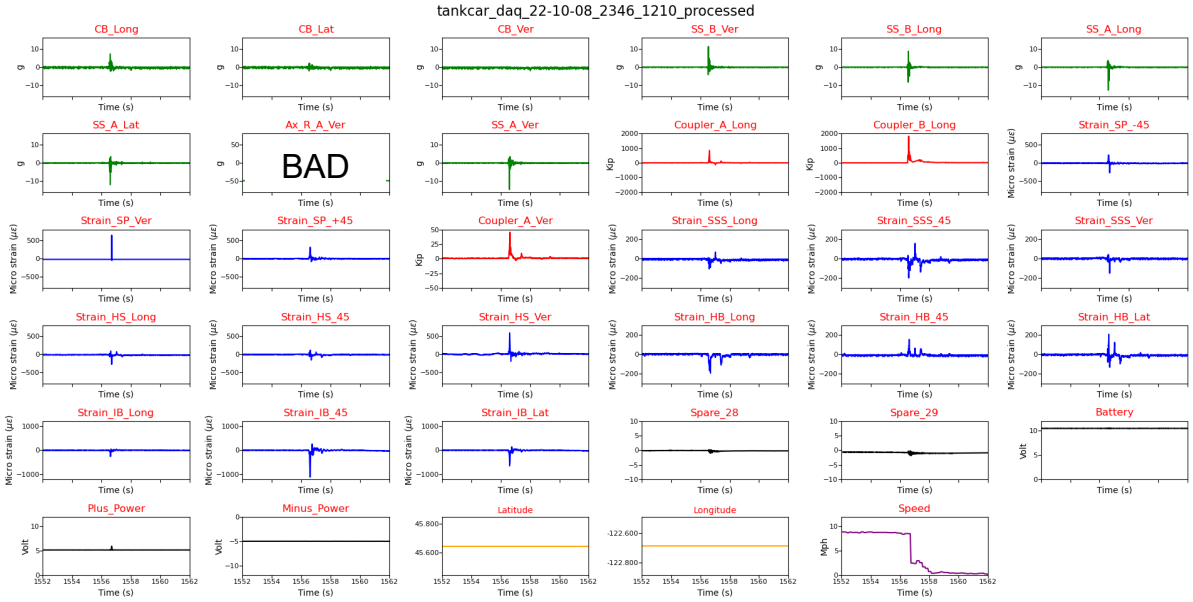

Figure 22. Magnified Plot with Highest Hard Longitudinal Coupler Forces (Yard 1, Magnified)

Figure 23 and Figure 24 plot the full file and magnified view of the second highest longitudinal coupler force for yard operations, respectively. Figure 25 and Figure 26 plot the full file and magnified view of the third highest longitudinal coupler force for yard operations, respectively. Figure 27 and Figure 28 plot the full file and magnified view of the fourth highest longitudinal coupler force for yard operations, respectively. All of these yard operation plots are indicative of yard movements as part of the train consist assembly.

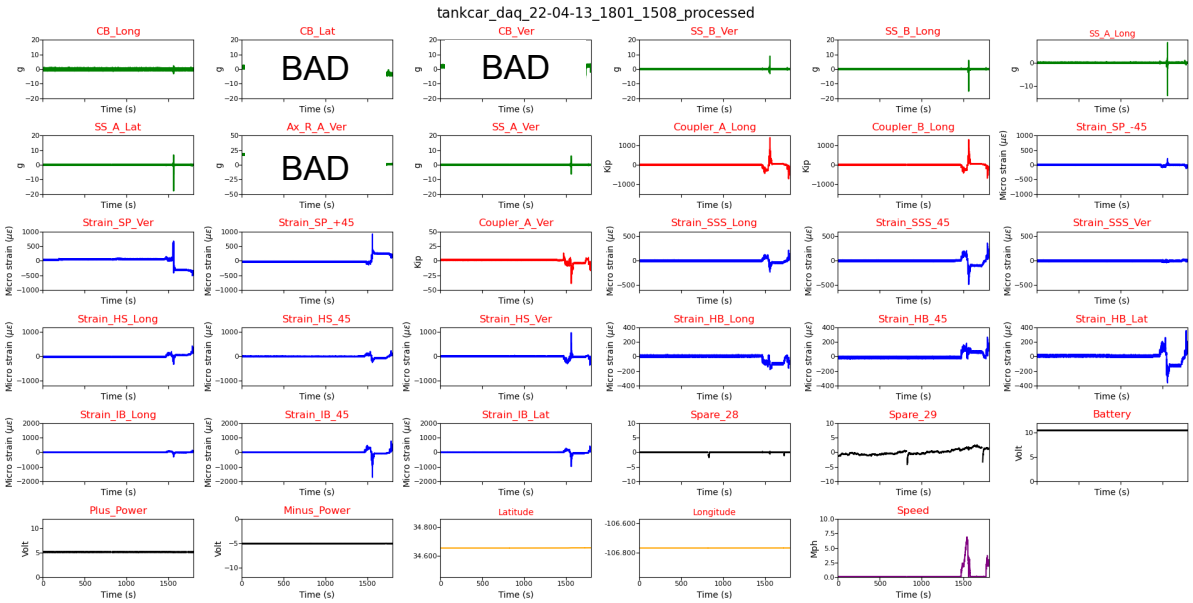

Figure 23. Plot with Second Highest Yard Longitudinal Coupler Forces (Yard 2, Full File)

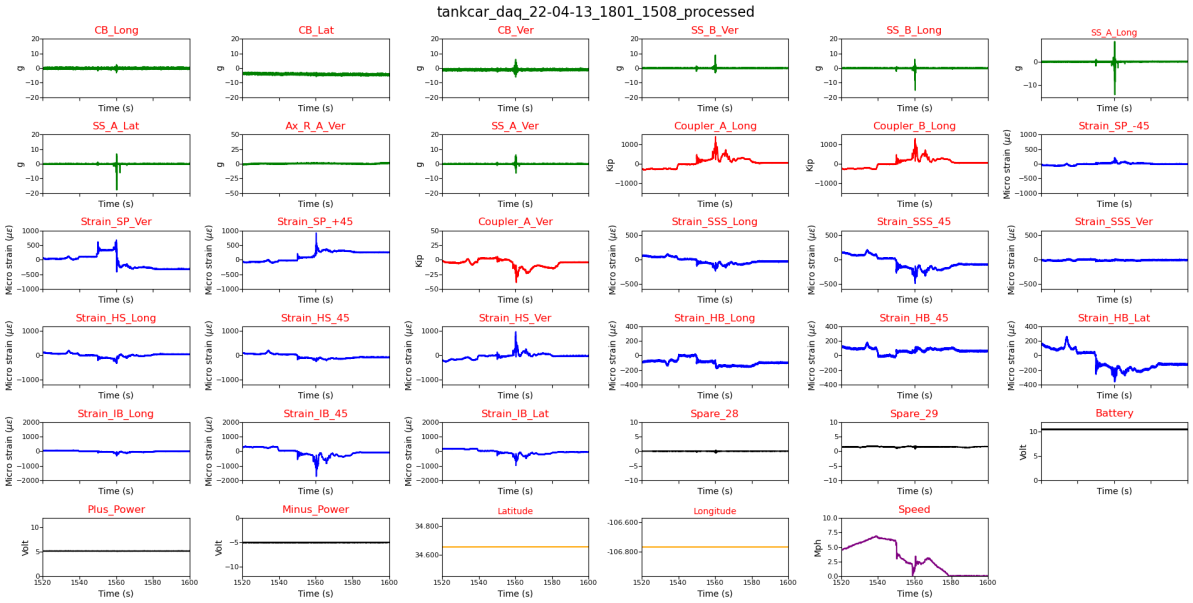

Figure 24. Zoomed-In Plot with Second Highest Yard Longitudinal Coupler Forces (Yard 2, Magnified)

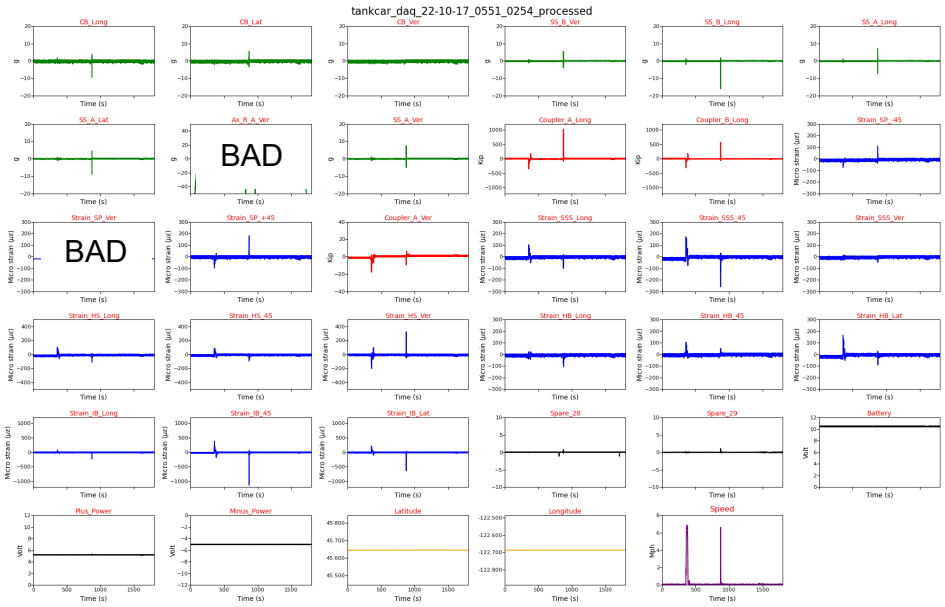

Figure 25. Plot with Third Highest Yard Longitudinal Coupler Forces (Yard 3, Full File)

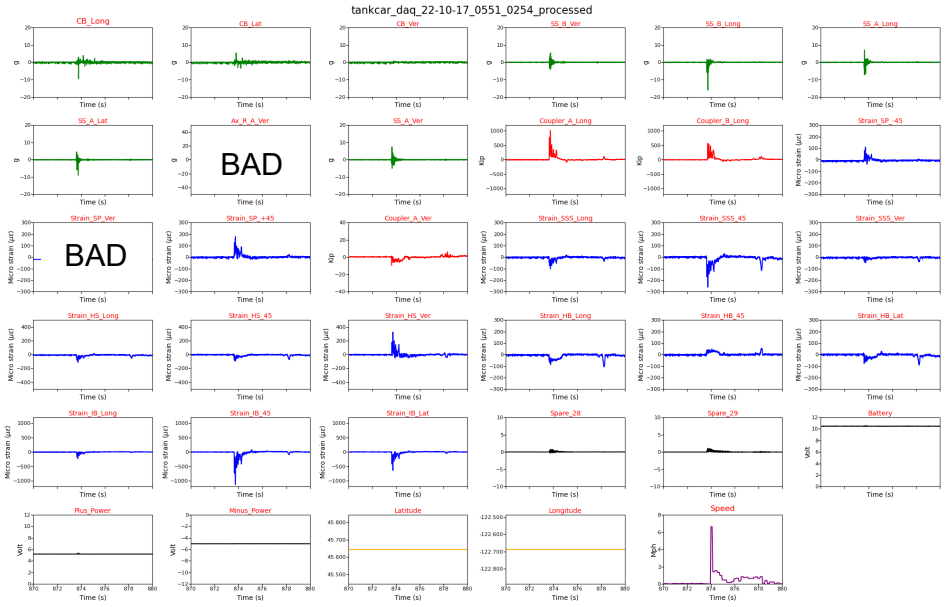

Figure 26. Zoomed-In Plot with Third Highest Yard Longitudinal Coupler Forces (Yard 3, Magnified)

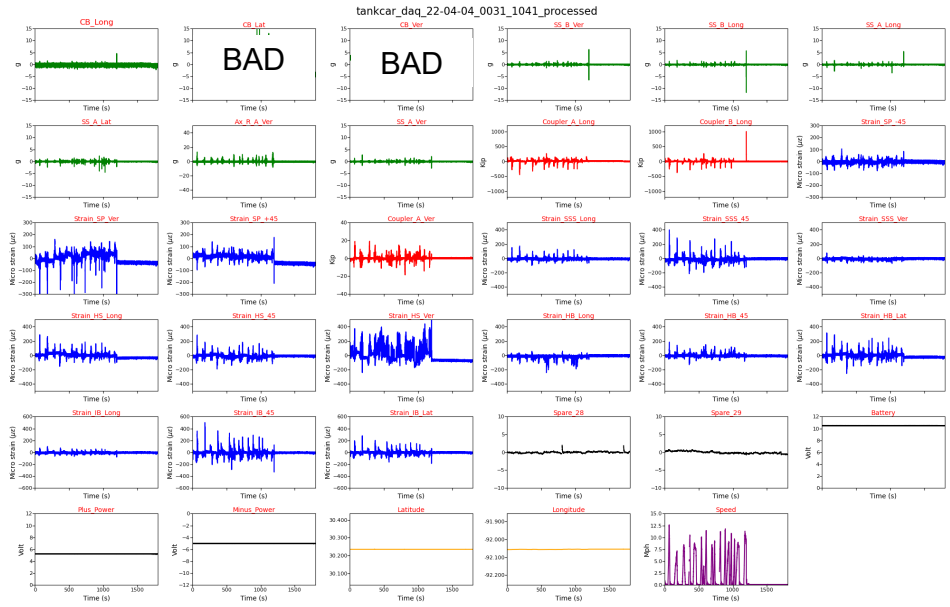

Figure 27. Plot with Fourth Highest Yard Longitudinal Coupler Forces (Yard 4, Full File)

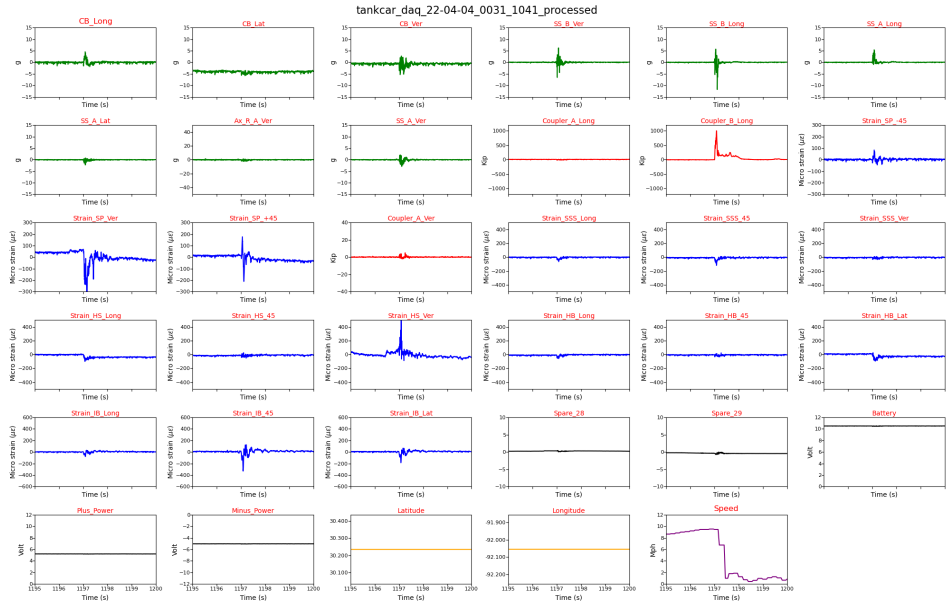

Figure 28. Zoomed-In Plot with Fourth Highest Yard Longitudinal Coupler Forces (Yard 4, Magnified)

Figure 29 and Figure 30 plot the full file and magnified view of the highest longitudinal coupler force for main operations, respectively. Figure 31 and Figure 32 plot the full file and magnified view of the second highest longitudinal coupler force for main operations, respectively. Figure 33 and Figure 34 plot the full file and magnified view of the third highest longitudinal coupler force for main operations, respectively. Figure 35 and Figure 36 plot the full file and magnified view of the fourth highest longitudinal coupler force for main operations, respectively. All of

these main operation plots show speed changes in normal mainline operation. These generally happen when the train is accelerating or on rare occasions when breaking.

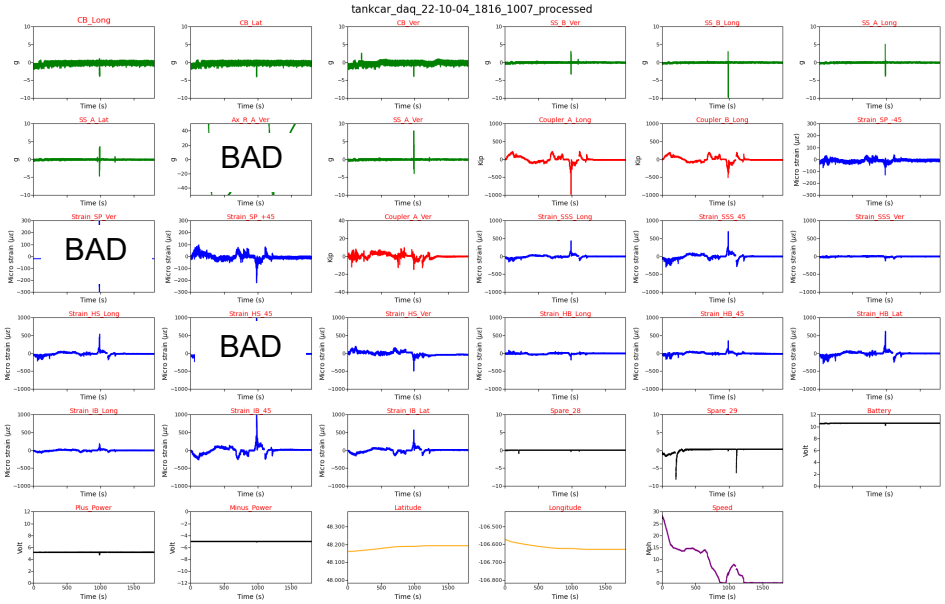

Figure 29. Plot with Highest Main Longitudinal Coupler Forces (Main 1, Full File)

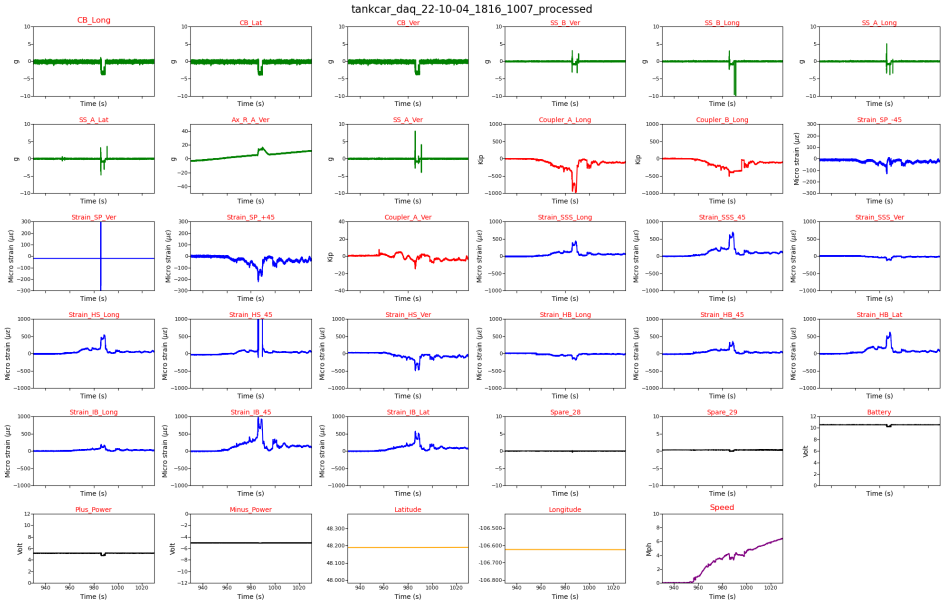

Figure 30. Zoomed-In Plot with Highest Main Longitudinal Coupler Forces (Main 1, Magnified)

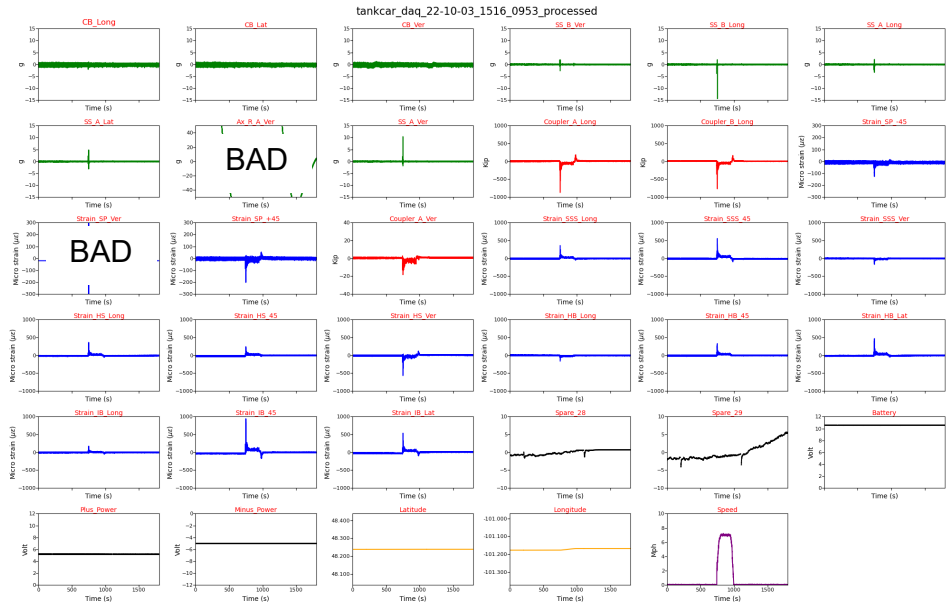

Figure 31. Plot with Second Highest Main Longitudinal Coupler Forces (Main 2, Full File)

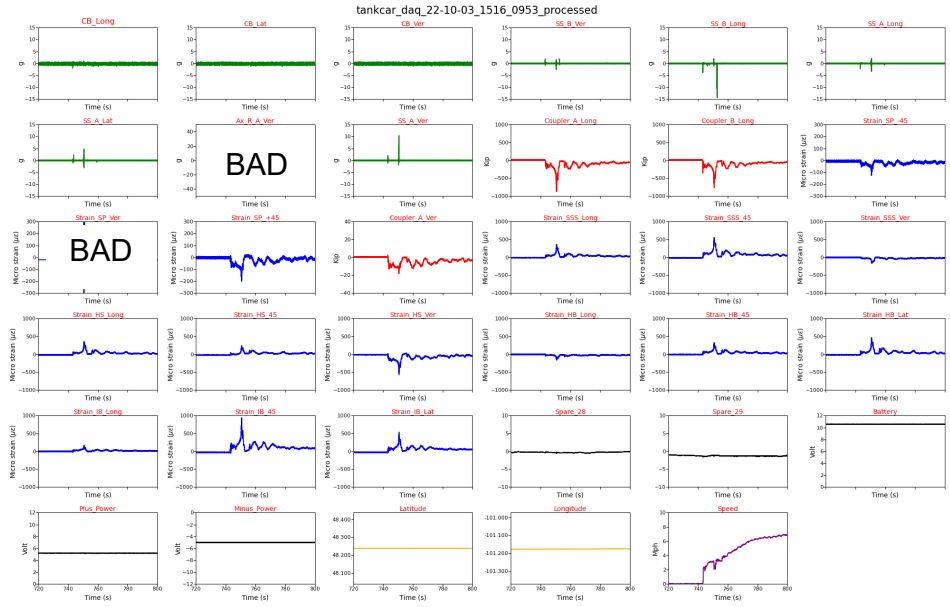

Figure 32. Zoomed-In Plot with Second Highest Main Longitudinal Coupler Forces (Main 2, Magnified)

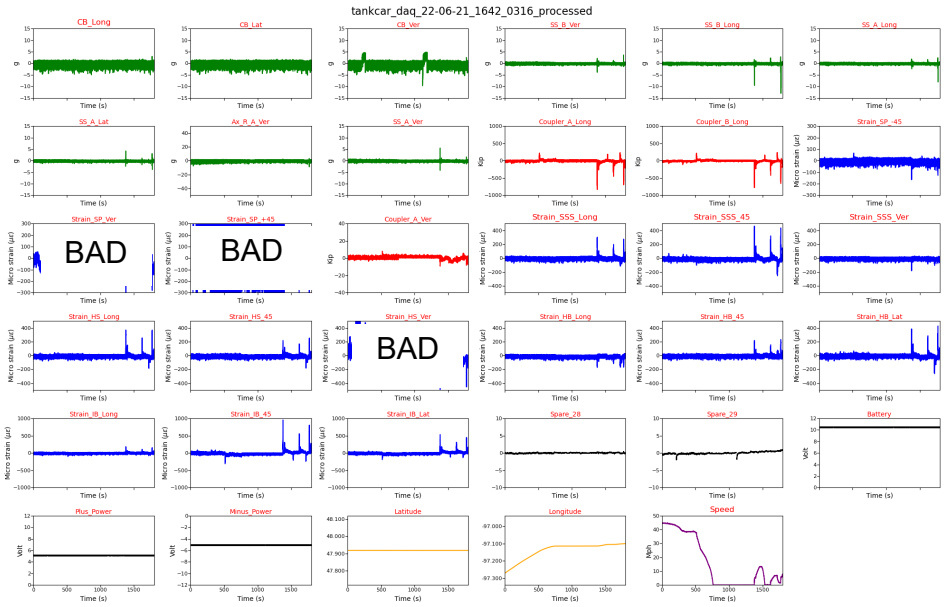

Figure 33. Plot with Third Highest Main Longitudinal Coupler Forces (Main 3, Full File)

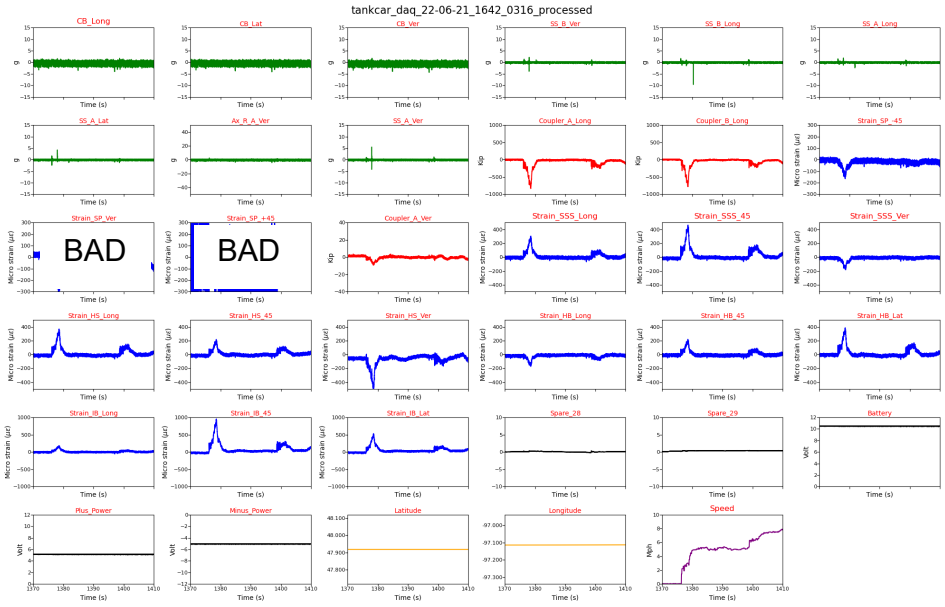

Figure 34. Zoomed-In Plot with Third Highest Main Longitudinal Coupler Forces (Main 3, Magnified)

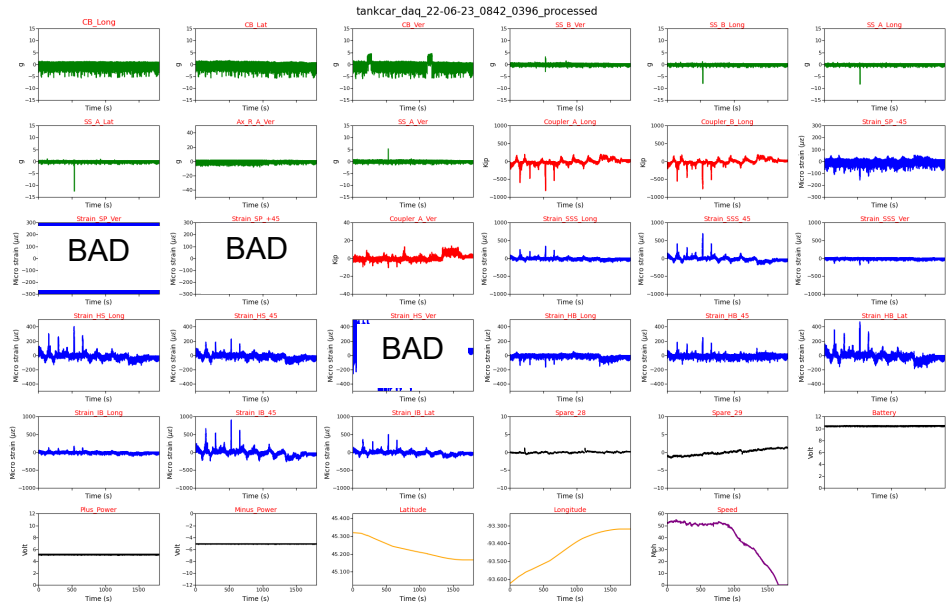

Figure 35. Plot with Fourth Highest Main Longitudinal Coupler Forces (Main 4, Full File)

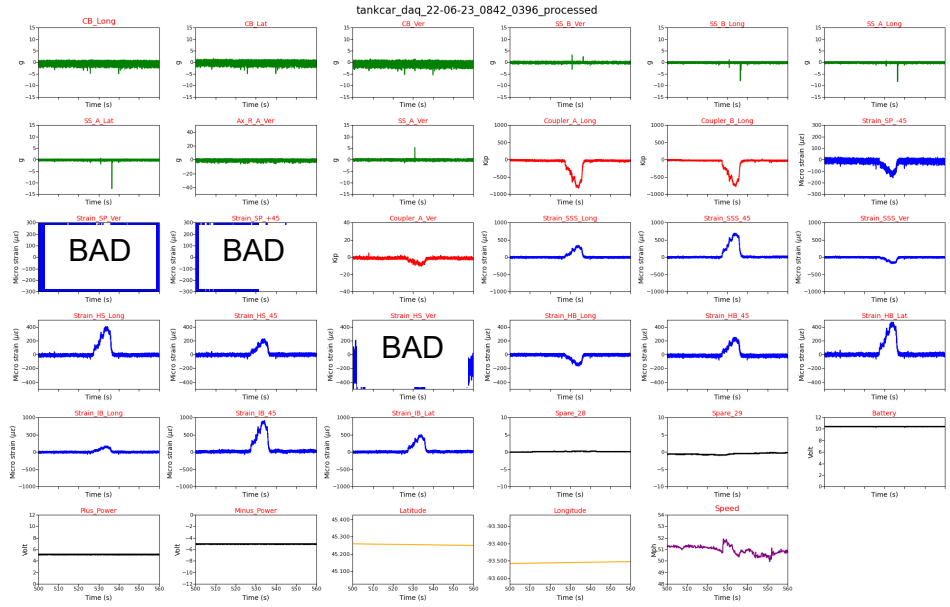

Figure 36. Zoomed-In Plot with Fourth Highest Main Longitudinal Coupler Forces (Main 4, Magnified)

3.4 Speed Analysis

In the next step of the analysis, the team investigated the peaks for each file to better understand the influence of the type of train operation and other factors. All data files were categorized as either main operation or yard operation as previously discussed. The various sensors were plotted versus date and color coded for the type of operation. Figure 37 shows the peak speeds for each file with the main operations in blue and the yard operations in red. The main operations had

peak speeds up to 67 mph with most of the mainline at peaks between 40 and 60 mph. The yard operations generally had peaks under 15 mph.

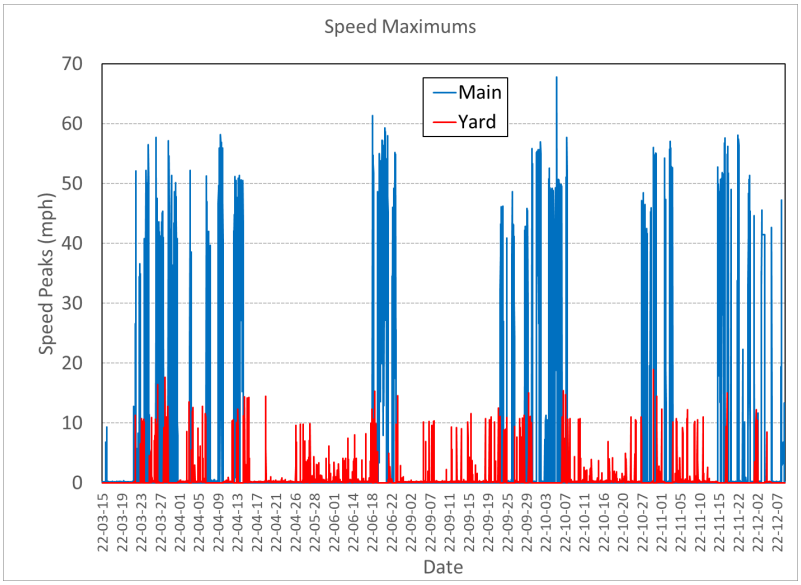

Figure 37. Maximum Speeds for Entire Test Program

3.5 Peak Acceleration Analysis

The team then analyzed the accelerations. Figure 38 shows the two stub sill longitudinal accelerations (the longitudinal direction was the most important for this analysis). The main operations are shown in blue while the yard operations are shown in red. This figure shows many large peaks for both main and yard operations. The data showed that there are many more negative peaks than positive peaks. It was presumed that the number of peaks would be roughly equal because it was assumed that the tank car would change its orientation in the train consist periodically at random. However, information on the tank car orientation was not available. It is possible that the autonomous testing was performed with the tank car in one prevalent orientation.

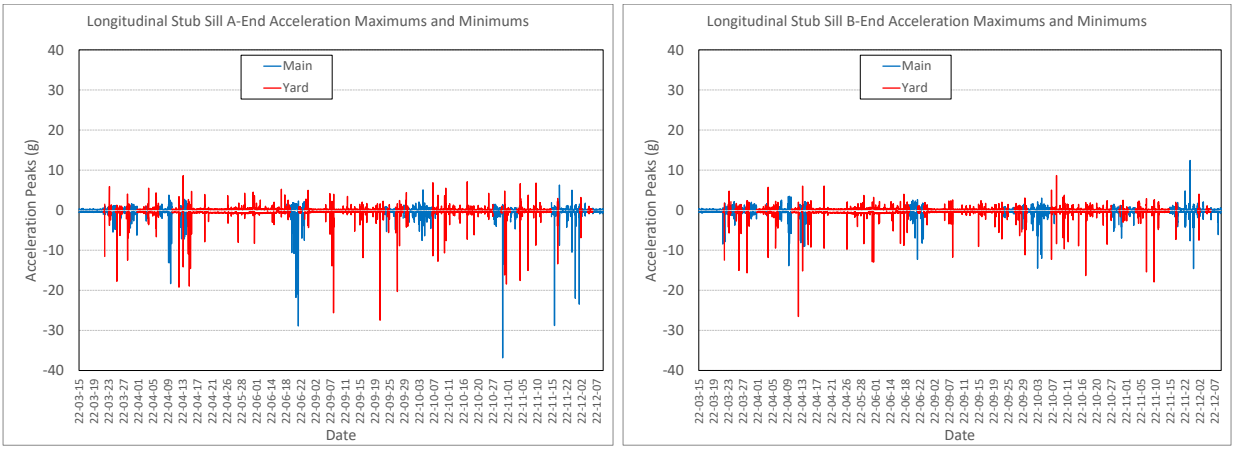

Figure 38. Stub Sill Longitudinal Acceleration Peaks (Left is A-End, Right is B-End)

3.6 Peak Force Analysis

One of the main factors affecting stub sill damage is the longitudinal coupler force. Figure 39 shows longitudinal coupler force peaks during the entire test program. The main operations are shown in blue while the yard operations are shown in red.

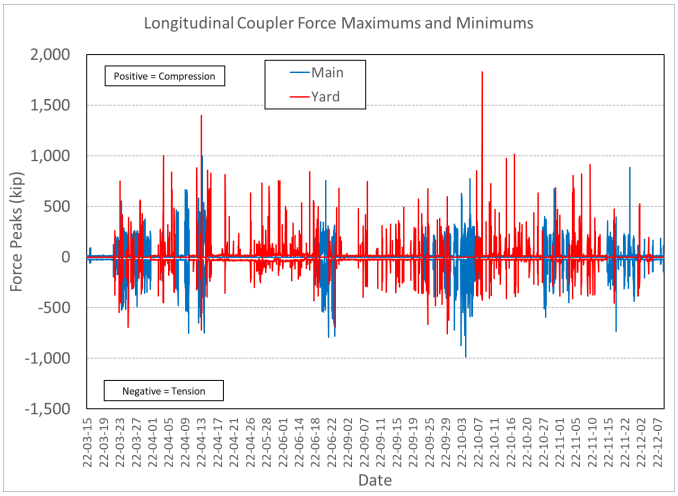

Figure 39. Longitudinal Coupler Force Peaks

Figure 40 shows a histogram of the longitudinal coupler forces and the worst 100 values. The main operations are shown in blue while the yard operations are shown in red. The histogram shows the number of events using a bin size of 50 kips and uses a log scale on the vertical axis for the counts. To get a better understanding of the highest values, the 100 worst values are also plotted.

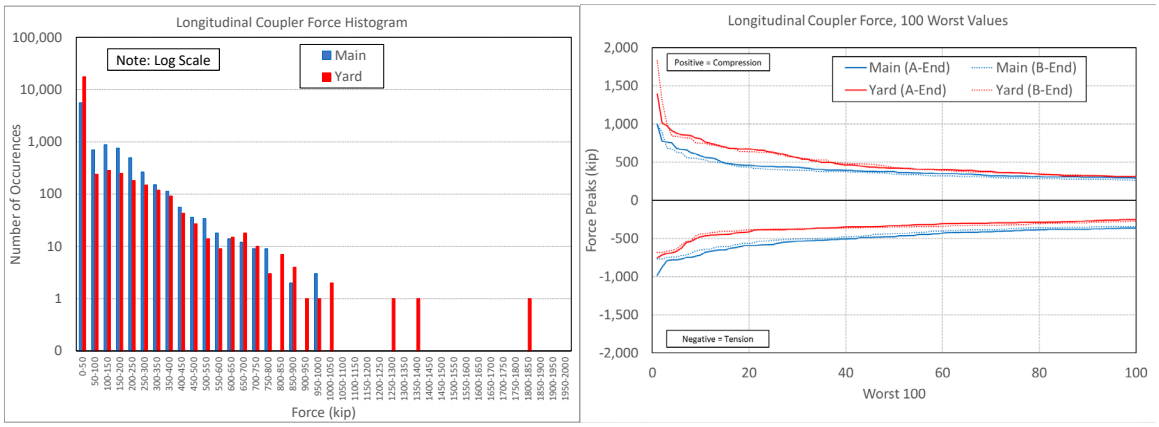

Figure 40. Longitudinal Coupler Force Histogram
(Left Shows Historam, Right Shows 100 Worst Values)

During the autonomous testing, the highest overall and the highest compression (i.e., positive) longitudinal coupler forces occurred during yard operations. Most of these events appear to be coupling actions as the railroads assemble the train consists.

The highest tension (i.e., negative) longitudinal coupler forces occurred during main operations. There were also many compression force events during main operations with similar magnitudes to the tension forces. These events appear to be train accelerations and braking actions.

Figure 41 shows box plots of the longitudinal coupler force for main and yard operations and compares it to the previous impact testing results. The main operations are still shown in blue while the yard operations are still shown in red. The impact testing is shown in green. Although box plots show many different statistical elements of the data, the main purpose here is to compare some of the actual worst-case values. These are shown using small circles for the data points. The autonomous testing showed levels of the worst case peak longitudinal coupler forces that were very similar to those in the previous impact testing .

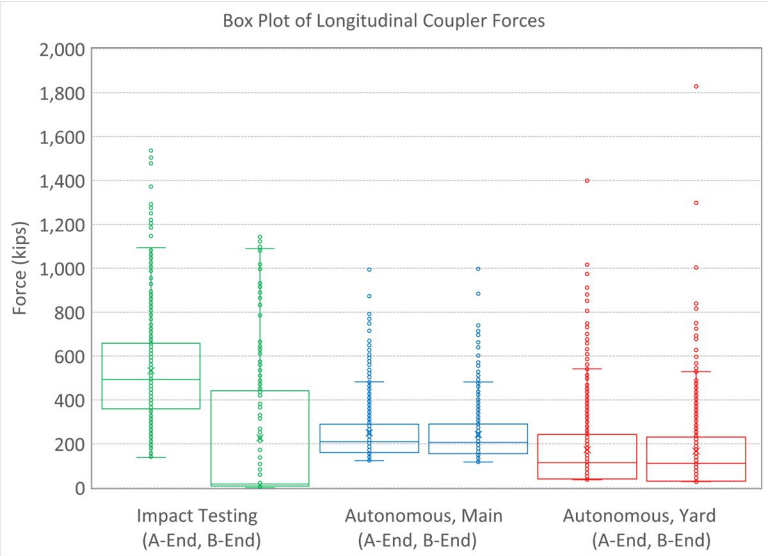

Figure 41. Longitudinal Coupler Force Box Plots with Impact Test Comparison

Another factor affecting stub sill damage is the vertical coupler force. Figure 42 shows vertical coupler force peaks during the entire test program. The main operations are shown in blue while the yard operations are shown in red.

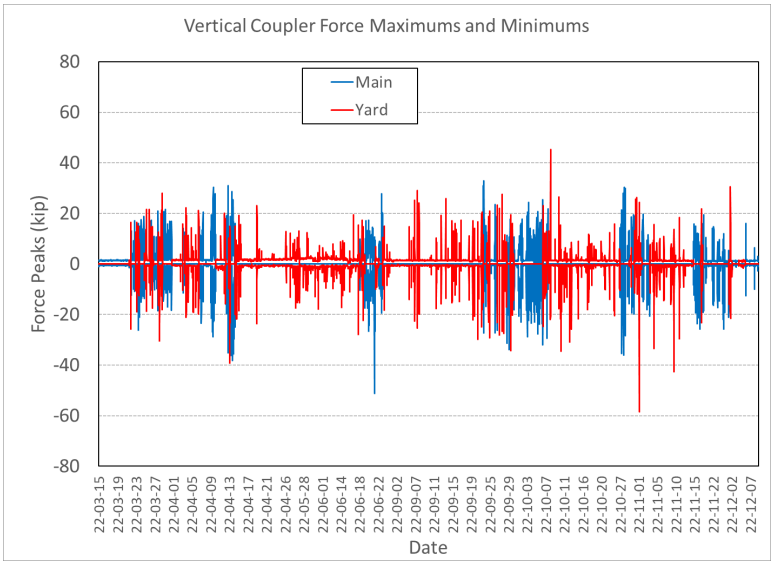

Figure 42. Vertical Coupler Force Peaks

Figure 43 shows a histogram of the vertical coupler force and the worst 100 values. The main operations are shown in blue while the yard operations are shown in red. The histogram shows

the number of events using a bin size of 2 kips and uses a log scale for the vertical axis showing the counts. To get a better understanding of the highest values, the 100 worst values are also plotted.

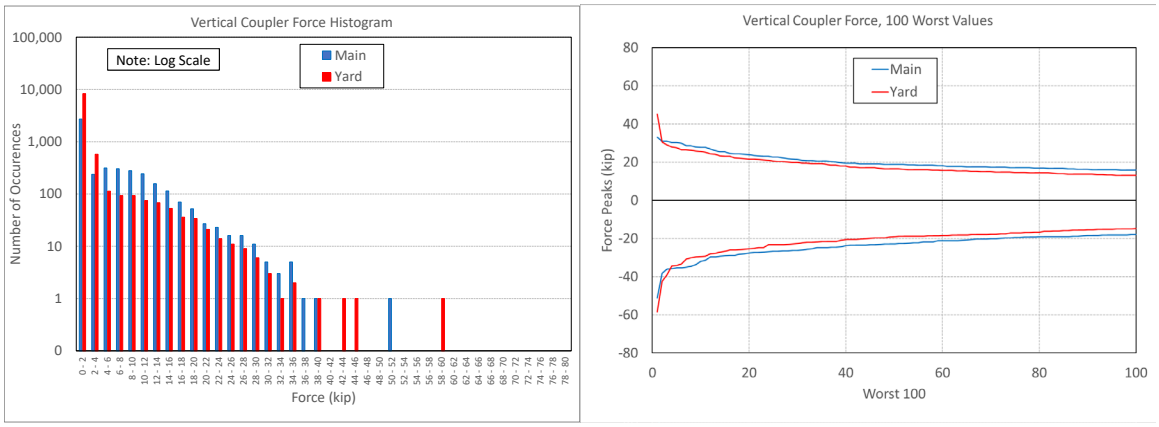

Figure 43. Vertical Coupler Force Histogram
(Left Shows Historam, Right Shows 100 Worst Values)

During the autonomous testing, the main and yard operations had similar levels of vertical coupler forces. The highest force occurred in yard operations, but main operations had slightly higher forces overall.

Figure 44 shows box plots of the vertical coupler force for main and yard operations and compares it to the previous impact testing results. The main operations are still shown in blue while the yard operations are still shown in red. The impact testing is shown in green. Although box plots show many different statistical elements of the data, the main purpose here is to compare some of the actual worst-case values. These are shown using small circles for the data points. The autonomous testing recorded approximately half the magnitude levels of the previous impact testing.

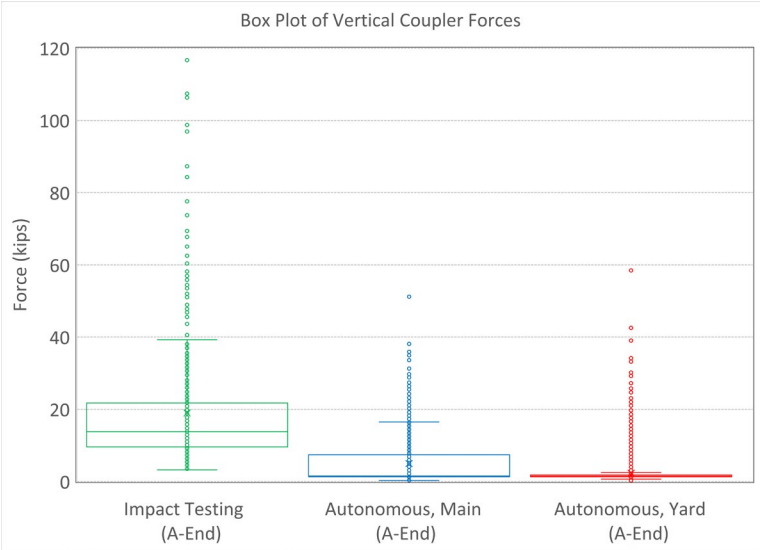

Figure 44. Vertical Coupler Force Box Plots with Impact Test Comparison

3.7 Peak Strain Analysis

The tank car was instrumented with five sets of rosette strain gauges placed at different locations around the stub sill that were identified as high stress locations. Figure 8 through Figure 12 previously seen in this report illustrate the strain gauges and their locations. Each rosette consisted of three uniaxial strain gages, resulting in fifteen strain gauge channels being recorded during testing. Each rosette was examined separately and then compared afterward.

Figure 45 shows the shoulder pad strain peaks during the entire test program. Figure 46 shows a histogram and the worst 100 values. The histogram shows the number of events using a bin size of 50 με and a log scale on the vertical axis for the counts. To get a better understanding of the highest values, the 100 worst values are also plotted. Figure 47 shows box plots for main and yard operations and compares them to the impact testing from the previous phase. Although box plots show many different statistical elements of the data, the main purpose here is to compare some of the actual worst-case values. These are shown using small circles for the data points. For these figures, main operations are shown in blue, yard operations are shown in red, and the previous impact testing is shown in green (where applicable).

During the autonomous testing, main and yard operations had similar levels of shoulder pad strain. The autonomous testing levels were approximately 50 percent higher than those in the previous impact testing.

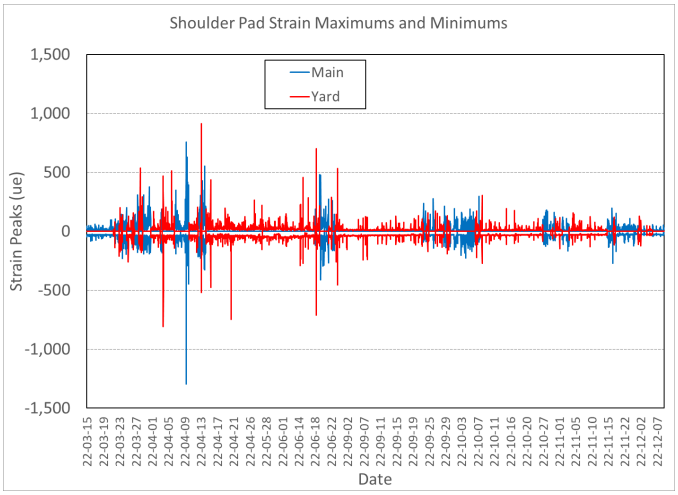

Figure 45. Should Pad Strain Peaks

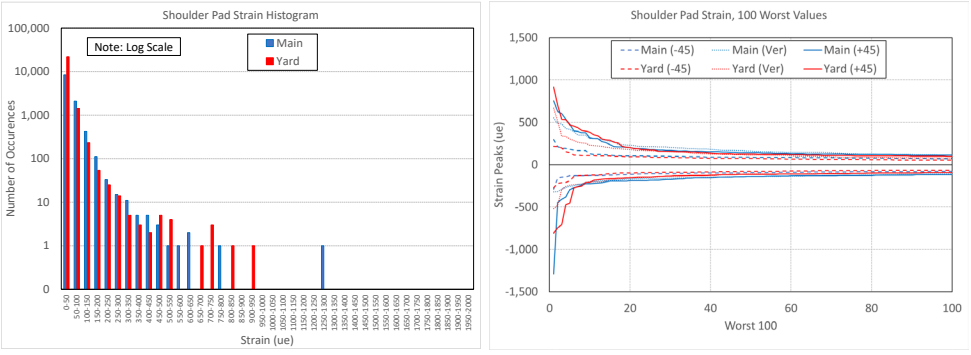

Figure 46. Shoulder Pad Strain Histogram
(Left Shows Historam, Right Shows 100 Worst Values)

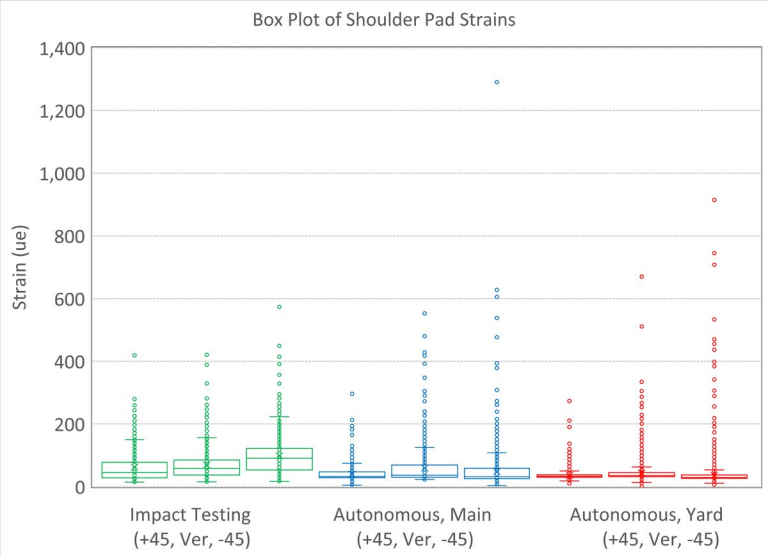

Figure 47. Shoulder Pad Strain Box Plots with Impact Test Comparison

Figure 48 shows the stub sill stop strain peaks during the entire test program. Figure 49 shows a histogram and the worst 100 values. The histogram shows the number of events using a bin size of 50 με and a log scale on vertical ais for the counts. To get a better understanding of the highest values, the 100 worst values are also plotted. Figure 50 shows box plots for main and yard operations and compares them to the impact testing from the previous phase. Although box plots show many different statistical elements of the data, the main purpose here is to compare some of the actual worst-case values. These are shown using small circles for the data points. For these figures, main operations are shown in blue, yard operations are shown in red, and the previous impact testing is shown in green (if applicable).

During the autonomous testing, main operations showed approximately 25 percent higher levels of stub sill stop strain than yard operations. The autonomous testing showed approximately 15 percent lower levels than the previous impact testing.

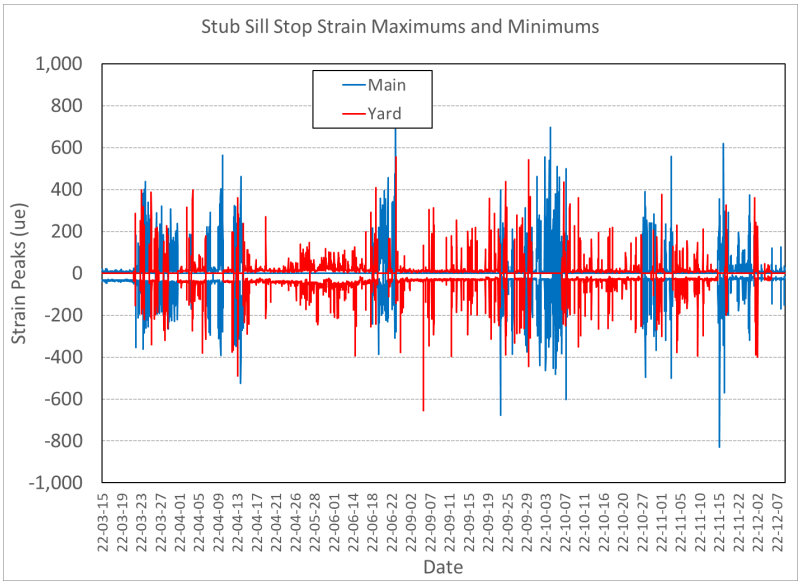

Figure 48. Stub Sill Stop Strain Peaks

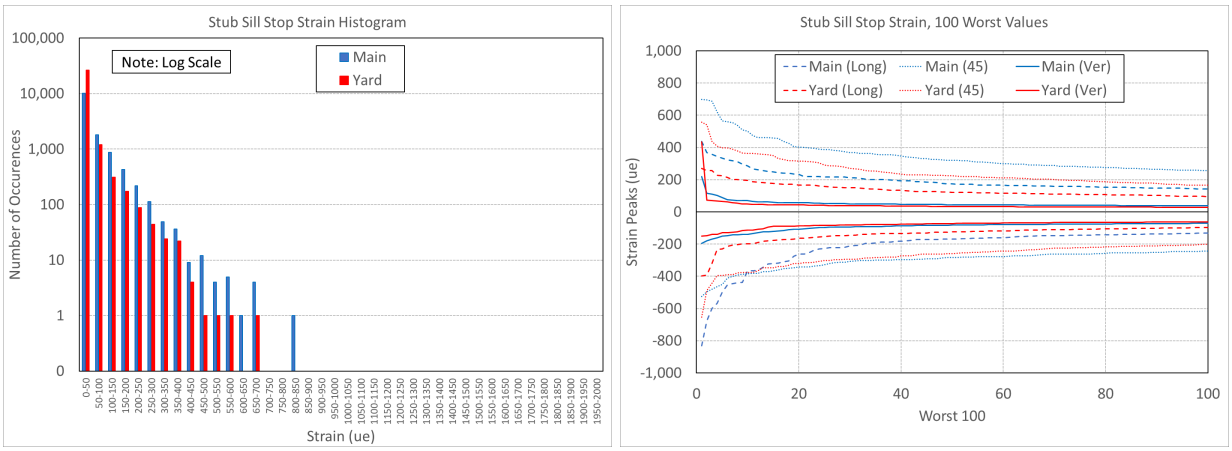

Figure 49. Stub Sill Stop Strain Histogram
(Left Shows Historam, Right Shows 100 Worst Values)

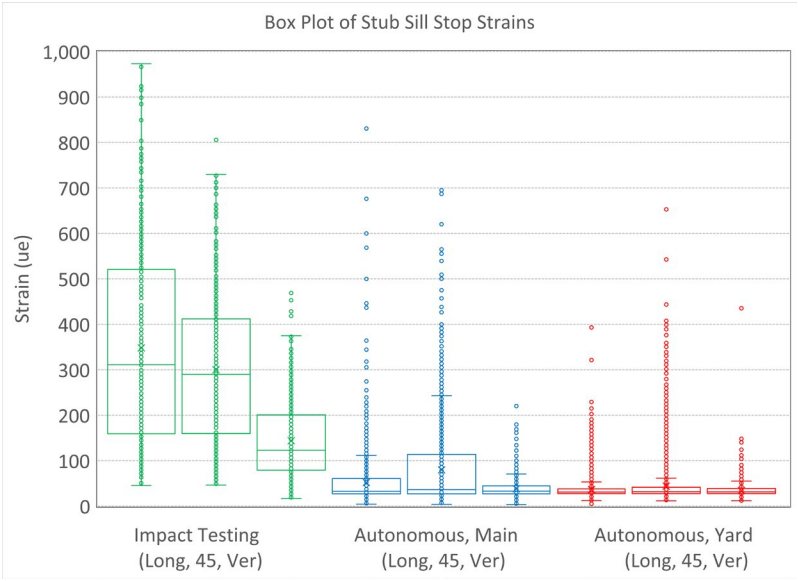

Figure 50. Stub Sill Stop Strain Box Plots with Impact Test Comparison

Figure 51 shows the head shoe strain peaks during the entire test program. Figure 52 shows a histogram and the worst 100 values. The histogram shows the number of events using a bin size of 50 με and a log scale on vertical axis for the counts. To get a better understanding of the highest values, the 100 worst values are also plotted. Figure 53 shows box plots for main and yard operations and compares them to the impact testing from the previous phase. Although box plots show many different statistical elements of the data, the main purpose here is to compare some of the actual worst-case values. These are shown using small circles for the data points. For these figures, the main operations are shown in blue, the yard operations are shown in red, and the previous impact testing is shown in green (if applicable).

During the autonomous testing, main operations showed approximately 25 percent higher levels of head shoe strain than yard operations. The autonomous testing had slightly lower levels than the previous impact testing.

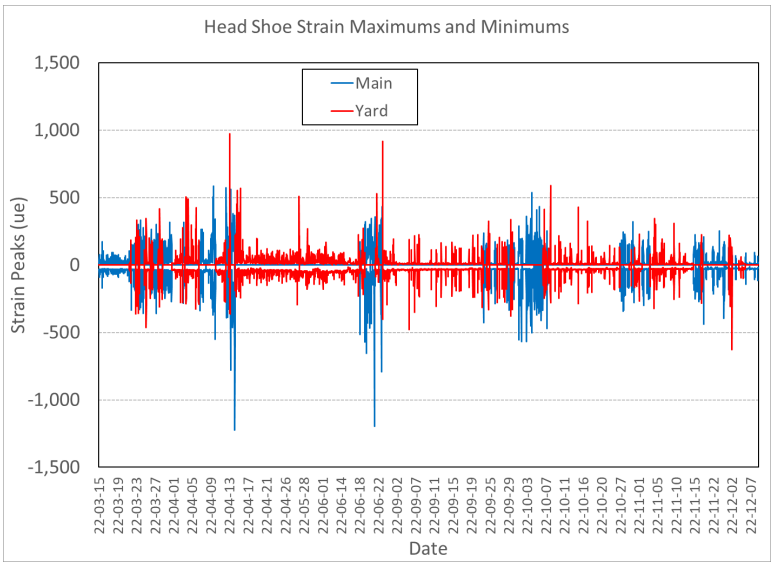

Figure 51. Head Shoe Strain Peaks

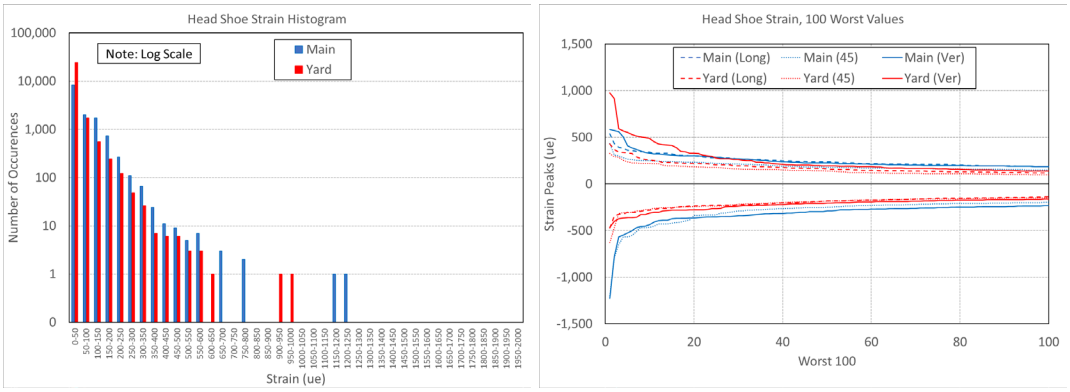

Figure 52. Head Shoe Strain Histogram
(Left Shows Historam, Right Shows 100 Worst Values)

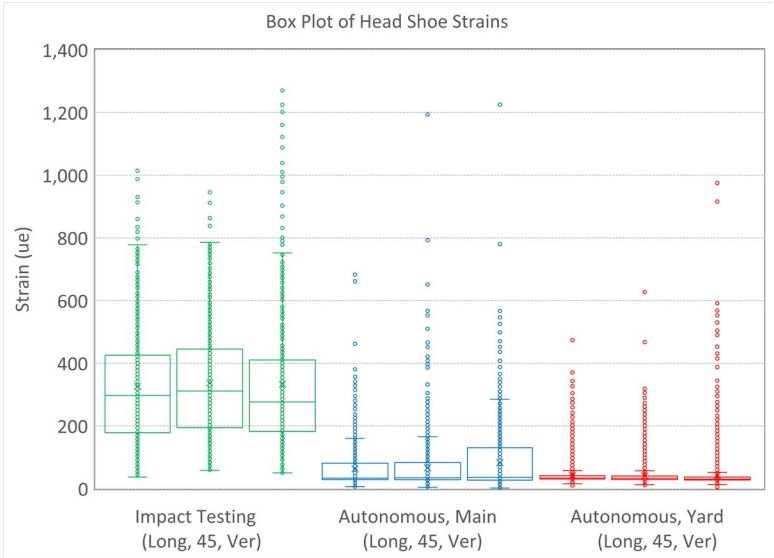

Figure 53. Head Shoe Strain Box Plots with Impact Test Comparison

Figure 54 shows the head brace strain peaks during the entire test program. Figure 55 shows a histogram and the worst 100 values. The histogram shows the number of events using a bin size of 50 με and a log scale on vertical axis for the counts. To get a better understanding of the highest values, the 100 worst values are also plotted. Figure 56 shows box plots for main and yard operations and compares them to the impact testing from the previous phase. Although box plots show many different statistical elements of the data, the main purpose here is to compare some of the actual worst-case values. These are shown using small circles for the data points. For these figures, main operations are shown in blue, yard operations are shown in red, and the previous impact testing is shown in green (if applicable).

During the autonomous testing, main and yard operations showed similar levels of head brace strain. The autonomous testing showed approximately 50 percent lower levels than the previous impact testing.

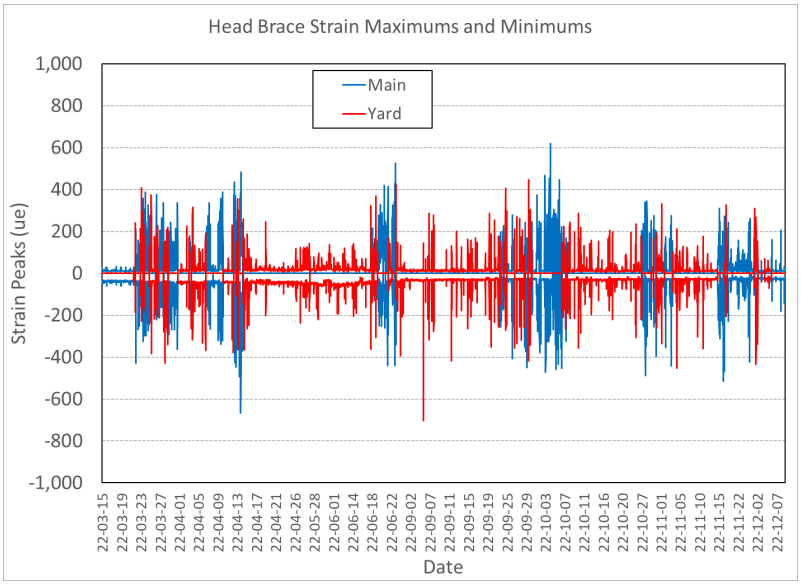

Figure 54. Head Brace Strain Peaks

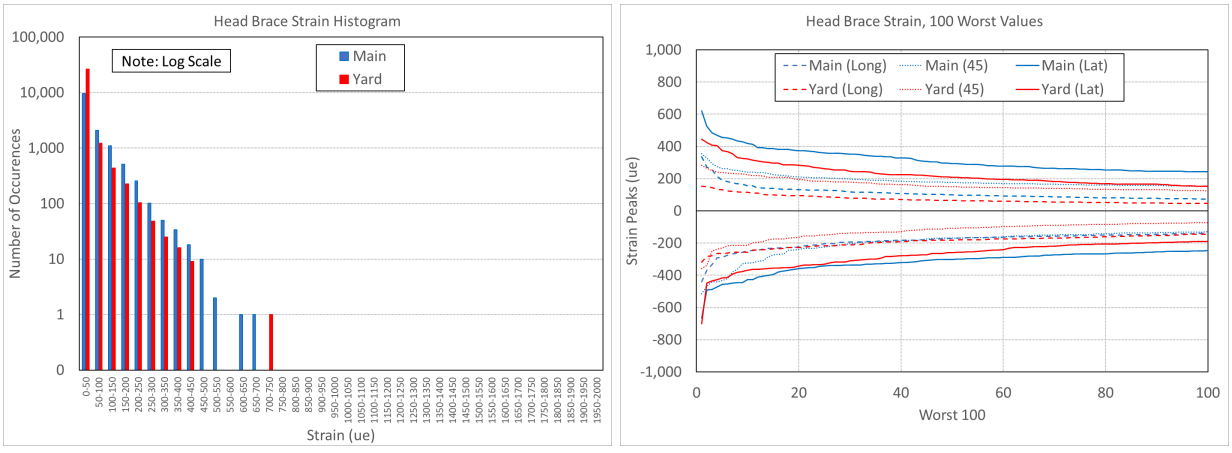

Figure 55. Head Brace Strain Histogram
(Left Shows Historam, Right Shows 100 Worst Values)

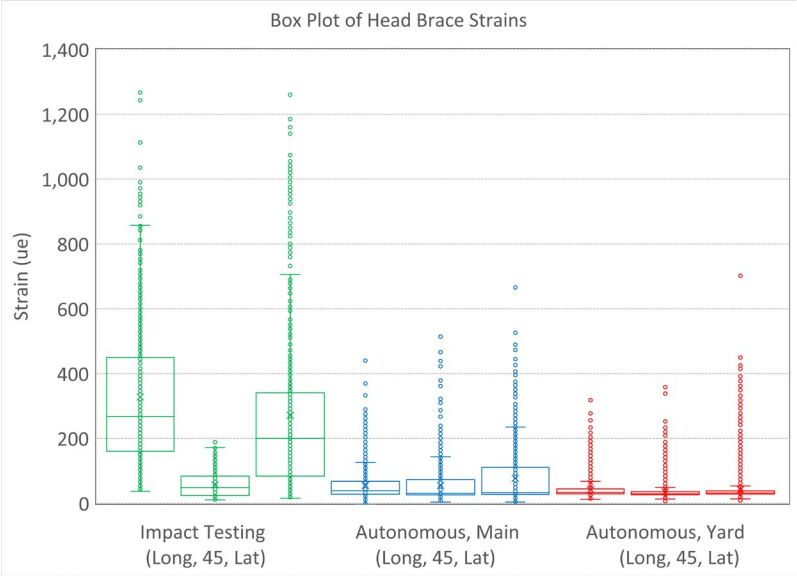

Figure 56. Head Brace Strain Box Plots with Impact Test Comparison

Figure 57 shows the in-board strain peaks during the entire test program. Figure 58 shows a histogram and the worst 100 values. The histogram shows the number of events using a bin size of 50 με and a log scale on vertical axis for the counts. To get a better understanding of the highest values, the 100 worst values are also plotted. Figure 59 shows box plots for main and yard operations and compares them to the impact testing from the previous phase. Although box plots show many different statistical elements of the data, the main purpose here is to compare some of the actual worst-case values. These are shown using small circles for the data points. For these figures, main operations are shown in blue, yard operations are shown in red, and the previous impact testing is shown in green (if applicable).

During the autonomous testing, yard operations showed approximately 50 percent higher levels of the in-board strain than main operations. The autonomous testing showed approximately 40 percent lower levels than the previous impact testing.

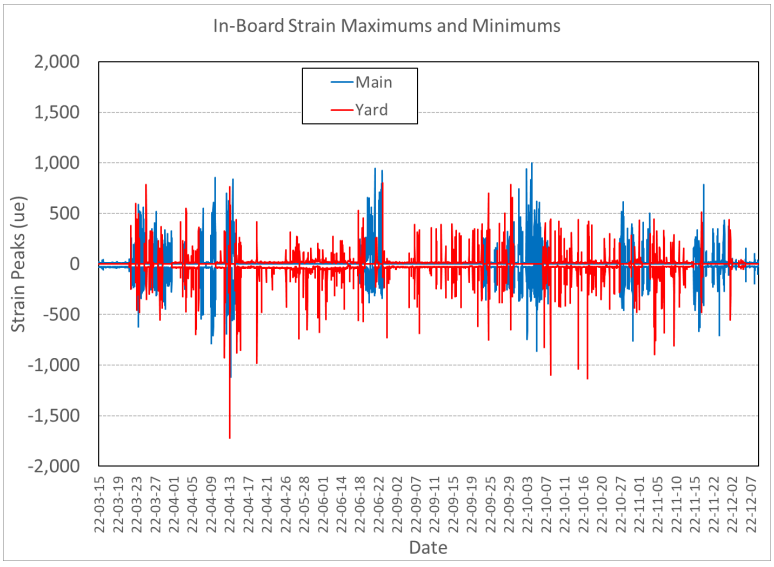

Figure 57. In-Board Strain Peaks

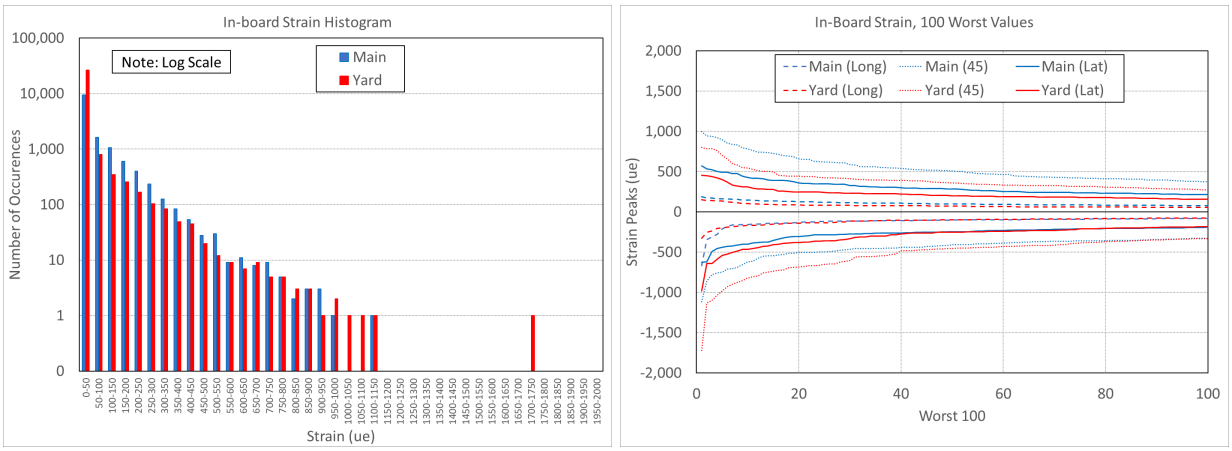

Figure 58. In-Board Strain Histogram
(Left Shows Historam, Right Shows 100 Worst Values)

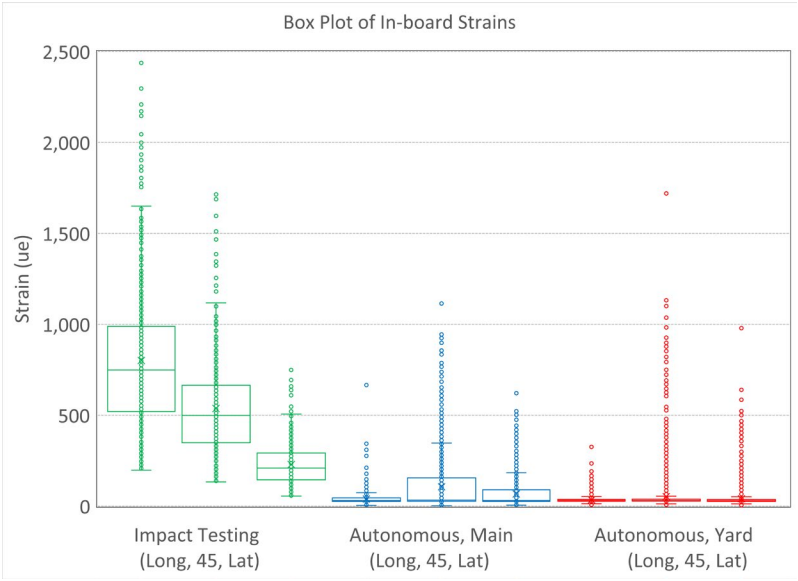

Figure 59. In-Board Strain Box Plots with Impact Test Comparison

Researchers also considered where the maximum strain occurs. Figure 60 shows the box plot for all five rosette strains (15 strain gauges) for main and yard operations during the autonomous testing. Each color shows the different rosettes with main operations on the left (the open circles) and yard operations on the right (the filled circles with the gray glow). The in-board strain showed the highest values. The shoulder pad and head shoe strains were in the middle with values approximately 30 percent lower. The stub sill stop and head brace strains were the lowest with values approximately 50 percent lower.

Figure 61 shows the box plot for the same five rosettes (15 strain gauges) for the previous impact testing. Each color is the same for each rosette as the previous figure of the autonomous testing. The in-board strains were the highest. The magnitudes for all the locations were different than the autonomous testing.

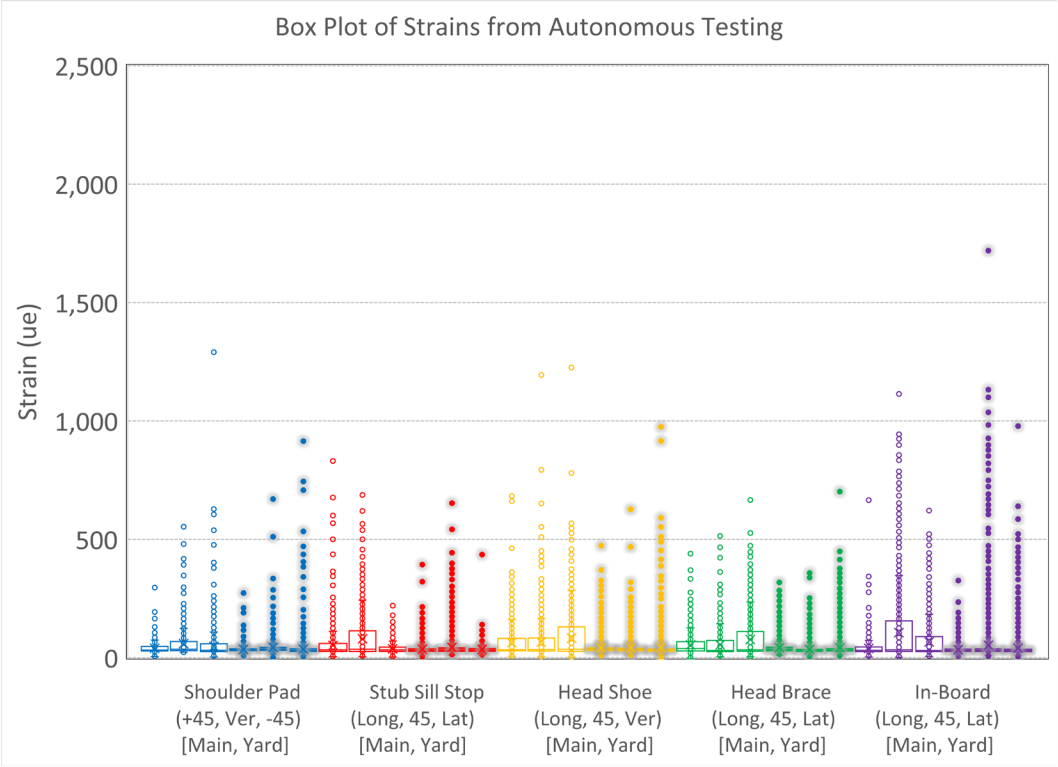

Figure 60. All Strain Box Plots for Autonomous Testing

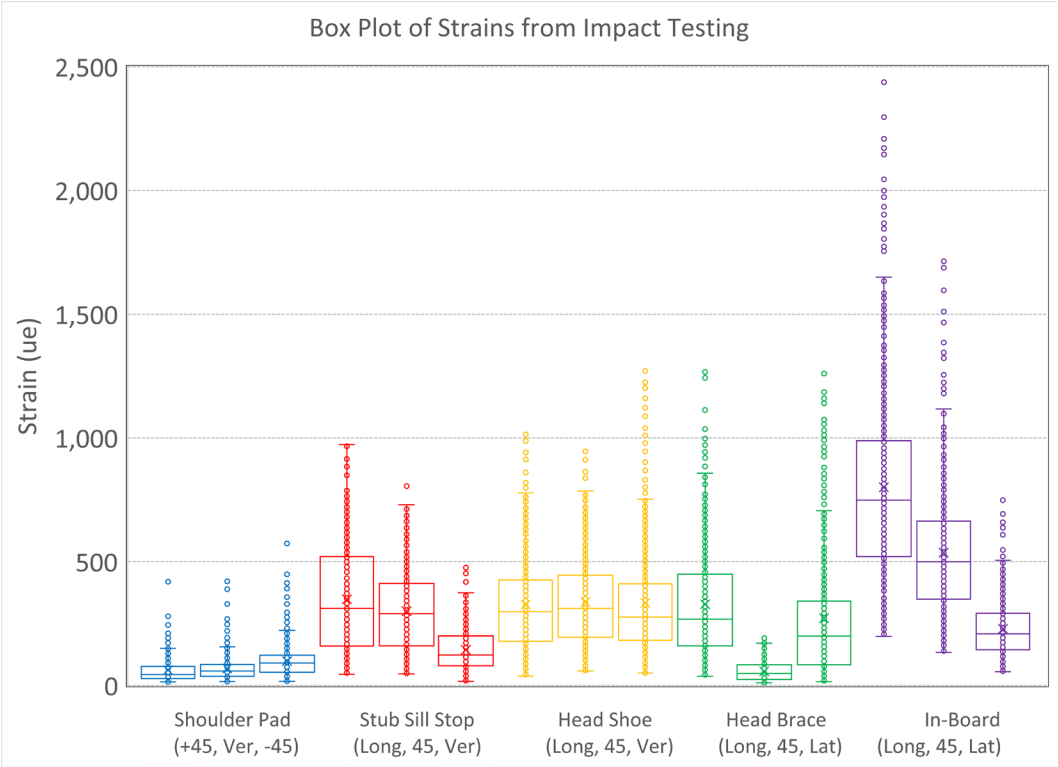

Figure 61. All Strain Box Plots for Impact Testing

4. Conclusion

The research team conducted a cooperative test program on Class I railroads across the United States in 2022. A tank car loaned to FRA by Union Tank Car was instrumented with multiple transducers and a data collection system that supported the high sampling rates required for revenue testing. The tank car ran in normal revenue service for 10 months and covered 14,000 miles of track, gathering acceleration, force, speed, and strain data. A comprehensive statistical data analysis was conducted to investigate the effect of various parameters, particularly the effect of mainline versus yard operations. The team drew the following major conclusions from the data analysis:

- Yard operations have slightly larger longitudinal coupler forces than main operations but similar magnitudes.
    - Yard operations have higher compression (i.e., positive) values (1830 kip maximum) than main operations (1000 kip maximum) due to coupling actions in switching yards.
    - Main operations have higher tension (i.e., negative) values (-980 kip maximum) than yard operations (-750 kip maximum) due to train accelerations and breaking.
- Longitudinal coupler forces showed similar magnitudes for both the autonomous testing (1830 kip maximum) and the previous impact testing (1540 kip maximum).
- Vertical coupler forces showed similar magnitudes for both main operations (51 kip maximum) and yard operations (58 kip maximum) but about half of that of the previous impact testing (117 kip maximum).
- The rosette strains showed similar magnitudes overall between main operations (670 με to 1110 με maximums) and yard operations (650 με to 1720 με maximums) with some locations higher and some lower.
- The rosette strains showed similar magnitudes between autonomous testing (650 με to 1720 με maximums) and the previous impact testing (570 με to 2440 με maximums) but also showed some variation (i.e., some locations higher and some lower).
- The in-board strain location had the highest values for both autonomous testing (1720 με maximum) and the previous impact testing (2440 με maximum).

This testing showed that the train dynamics from mainline and yard operations are nearly equally important for longitudinal coupler forces and the resulting stub sill strains. This finding will help determine important areas of future research and identify recommendations for the railroads to improve safety. Part of this process should be improvements to both mainline and yard operation scenarios.

5. References

1. ENSCO, Inc. (2009). *Over-the-Road Testing of the Instrumented Tank Car – A Load Environment Study* (Report No. DOT/FRA/ORD-10/04). FRA.

2. Meymand, Sajjad (2019). *Impact Test Data Analysis for Load Environment Characterization of Tank Car Stub Sill During Yard Operations* (Report No. DOT/FRA/ORD-20/09). FRA.

3. Sundaram, N. (2014). *Force Environment Evaluation of Stub Sills on Tank Cars Using Autonomous Over-the-Road Testing of the Instrumented Tank Car* (Report No. DOT/FRA/ORD-16/39). FRA.

Abbreviations and Acronyms

ACRONYM	DEFINITION
ENSCO	ENSCO, Inc.
FRA	Federal Railroad Administration